



PONTIFICIA UNIVERSIDAD CATOLICA DE CHILE  
ESCUELA DE INGENIERIA

**SYNTHETIC WIND DATA SERIES FOR  
THE CHILEAN WIND PARK ANALYSIS:  
STUDY OF VARIABILITY, WIND  
ENERGY GENERATION AND CAPACITY  
FACTOR ESTIMATION**

**DANILO ANDRÉS JARA AGUILERA**

Tesis para optar al grado de  
Magister en Ciencias de la Ingeniería

Profesor Supervisor:  
**DAVID WATTS C.**

Santiago de Chile, (Marzo, 2012)

© 2012, Danilo Andrés Jara Aguilera



PONTIFICIA UNIVERSIDAD CATOLICA DE CHILE  
ESCUELA DE INGENIERIA

**SYNTHETIC WIND DATA SERIES FOR THE  
CHILEAN WIND PARK ANALYSIS: STUDY OF  
VARIABILITY, WIND ENERGY GENERATION  
AND CAPACITY FACTOR ESTIMATION**

**DANILO ANDRÉS JARA AGUILERA**

Tesis presentada a la Comisión integrada por los profesores:

**DAVID WATTS**

**HUGH RUDNICK**

**LUIS LJUBETIC**

**JUAN DE DIOS RIVERA**

Para completar las exigencias del grado de  
Magister en Ciencias de la Ingeniería

Santiago de Chile, (Marzo, 2012)

## AGRADECIMIENTOS

Quiero agradecer a mi amada esposa, por todo el apoyo, comprensión y amor que me entregó durante este proceso, dándome ánimo cuando más lo necesitaba y entusiasta apoyo en mis logros y éxitos. Sin ti, nada de esto habría sido posible.

Quiero agradecer además a mis padres y a mi hermana, a mis queridos suegros y cuñados, por siempre estar ahí con su amor incondicional, por ser una gran familia para mí y entregarme las herramientas, la voluntad y la fortaleza para llevar a buen término mis metas profesionales.

Quiero agradecer también el invaluable apoyo del profesor David Watts, quien dedicó muchas horas enseñándome y apoyándome en el desarrollo de mi tesis. El profesor Watts ha significado para mí un gran maestro y referente profesional, siendo estos años de trabajo junto a él un tiempo fructífero, grato y enriquecedor. Agradezco sus consejos y experiencias, los cuales guardaré para el futuro que se avecina.

Quiero agradecer además al Ingeniero Luis Ljubetic, ya que fueron sus enseñanzas en mis últimos años de pregrado las que me acercaron al estudio de la problemática energética y en especial de las energías renovables.

No quiero dejar fuera el importante apoyo entregado por Betty, Gianina, Jessica, Virginia, Carlos, amigos y compañeros de oficina, y a todo el cuerpo docente y administrativo del departamento de ingeniería eléctrica, por facilitar mi trabajo y entregarme momentos gratos durante mi estadía en el departamento.

Finalmente, quiero agradecer a Dios, por estar siempre junto a mí y mostrarme desde muy joven el camino que debía seguir, acompañándome en las importantes decisiones que tuve que tomar.

Para las grandes mujeres y hombres  
que han sido el pilar fundamental en  
mi vida: Dayann, mamá Rosa, papá  
Baldo, Nicole, tía Meli, tío Martín,  
Ly y Mané.

## ÍNDICE GENERAL

	Pág.
AGRADECIMIENTOS .....	iii
ÍNDICE GENERAL.....	v
ÍNDICE DE TABLAS .....	vii
ÍNDICE DE FIGURAS .....	viii
RESUMEN.....	x
ABSTRACT .....	xii
1. INTRODUCTION .....	1
2. CURRENT ENERGY SCENARIO AND THE WIND ROLE.....	3
2.1. A breakdown of the Chilean energy matrix .....	3
2.2. Chilean projects on wind power.....	6
2.3. Wind energy and how it is coping with the SIC demand.....	8
3. MEASUREMENTS AND THE CHILEAN WIND RESOURCE.....	10
3.1. Wind zones and measurements .....	13
3.2. Summary of the Wind Survey .....	14
3.3. Time frame of measurement .....	16
3.4. The wind Average monthly profile .....	16
3.5. The wind average daily profile.....	19
3.6. Wind rose for the power frequency and density .....	20
3.7. Vertical wind shear profile.....	22
3.8. Empiric and adjusted distribution of Weibull's statistical resource probability .....	26
4. AVAILABLE ENERGY AT THE SURVEYED AREAS.....	28
5. SEASONAL BEHAVIOR OF WIND RESOURCE.....	32

5.1.	Main components in the Wind Speed Behaviour .....	32
5.2.	Frequency spectrum for the wind resource: Kolmogorov spectrum .....	34
6.	WIND RESOURCE MODELLING USING AUTOREGRESSIVE MODELS	35
6.1.	Typical modelling in wind resource evaluation: Weibull distribution....	35
6.2.	Wind speed modeling using Autoregressive models .....	37
6.2.1.	Autoregressive models.....	38
7.	ADDING WIND POWER PLANTS AND REDUCING VARIABILITY.....	39
7.1.	Spatial correlation and variability of wind generation .....	40
8.	GENERATION OF SYNTHETIC DATA AND CALCULATION OF AGGREGATE POWER OF WIND FARMS .....	42
8.1.	Data .....	42
8.1.1.	Series de tiempo para la velocidad del viento.....	43
8.1.2.	Agenda of wind projects in Chile .....	46
8.1.3.	Mesoscale data and georeferencing .....	48
8.2.	Assumptions considered.....	49
8.3.	Procedure and modelling.....	51
8.3.1.	Wind data series and mesoscale information analysis.....	51
8.3.2.	Synthetic data generation.....	52
8.3.3.	Calculation of electricity generation for wind parks.....	55
8.4.	Results and discussion.....	56
8.4.1.	Wind power aggregation.....	60
8.4.2.	Capacity factor estimation .....	66
9.	CONCLUSIONS .....	68
	BIBLIOGRAFÍA.....	72

## ÍNDICE DE TABLAS

	Pág.
Table 2.1 – SIC’s installed capacity - April 2009 .....	4
Table 2.2 - SING’s installed capacity - April 2009.....	5
Table 3.1– Summary table of the main features at each measuring position.....	15
Table 3.2 – Monthly maximum and minimum wind speed readings at 61.5 m.....	17
Table 3.3 – Annual statistical data for the specific location readings.....	18
Table 3.4 – Daily maximum and minimum wind speed readings in the various locations included in the survey .....	20
Table 3.5 – Parameters for the shearing profile in each location.....	24
Table 3.6 – Weibull parameters for the carried out measurements.....	27
Table 8.1– Principal information about wind speed measurement locations in the northern and central Chile .....	44
Table 8.2 - Annual Statistics for measurement stations (Watts & Jara, 2011) .....	45
Table 8.3 - Principal information about wind energy projects modeled.....	48
Table 8.4 - Reference information for the projects modeled including mesoscale map .....	49
Table 8.5 - Statistical parameter for a real and corresponding synthetic wind data .....	59
Table 8.6 - Max and null generation number of hour for a wind park, a group of parks and the total in the country .....	62
Table 8.7 - Capacity factor for a wind farm, a group of wind farms (12) and the total for the country.....	66
Table 8.8 - Detailed information for project modeled: Installed capacity, capacity factor and average power.....	67

## ÍNDICE DE FIGURAS

	Pág.
Figure 2-1– Percentage breakdown of SIC’s installed capacity – April 2009 .....	5
Figure 2-2 – Percentage breakdown of SING’s installed capacity .....	5
Figure 2-3 – Continental Chile and her power systems .....	6
Figure 2-4 – Average annual generation and wind power generation in the SIC grid, year 2008.....	9
Figure 2-5 - Duration graphs for consumption and wind power generation in the SIC grid. ....	9
Figure 3-1 – Annual average speeds: Carrizalillo (a), Cebada Costa (b), Cerro JP (c), Faro Carranza (d), Lengua de Vaca (e), Llano de Chocolate (f), Loma del Hueso (g), Los Choros (h).....	11
Figure 3-2 – Daily average speeds: Carrizalillo (a), Cebada Costa (b), Cerro JP (c), Faro Carranza (d), Lengua de Vaca (e), Llano de Chocolate (f), Loma del Hueso (g), Los Choros (h).....	12
Figure 3-3 – Location of the measurement sites and associated milestones .....	15
Figure 3-4 - Shearing profile for each location.....	23
Figure 3-5 – Prevalent wind direction during 2007: Carrizalillo (a), Cebada Costa (b), Cerro JP (c), Faro Carranza (d), Lengua de Vaca (e), Llano de Chocolate (f), Loma del Hueso (g), Los Choros (h).....	24
Figure 3-6 – Wind speed frequency with fitted Weibull distribution in all station at 61.5 m for year 2007:: Carrizalillo (a), Cebada Costa (b), Cerro JP (c), Faro Carranza (d), Lengua de Vaca (e), Llano de Chocolate (f), Loma del Hueso (g), Los Choros (h).....	25
Figure 3-7 – Wind rose for energy density: Carrizalillo y Faro Carranza: Carrizalillo (a), Faro Carranza (b) .....	26
Figure 4-1 – Power curve of the REPower MD77 generator with a 1,525 kW rating ...	29
Figure 4-2 - The capacity factors for various data reading locations as opposed to the readings at the “Canela” wind farm. ....	31

Figure 5-1- Average monthly profile for locations: Carrizalillo (izq.), Cebada Costa (cen.), Cerro JP (der.) .....	33
Figure 5-2 – Periodogram for average wind speed for a year (left) and for power generation of one wind farm (Right).....	35
Figure 7-1 – Probability distribution for hourly power generation for a wind farm for an entire year .....	39
Figure 7-2 – Power curve for a wind generator (REPower MD77 generator with a 1,525 kW rating) .....	40
Figure 8-1 – Map of Chile including general description about wind projects modeled .....	47
Figure 8-2 - Wind Trajectories for real data (up) and synthetic data (down) in m/s .....	57
Figure 8-3 - Probability distribution (left) and daily profile (left) for real and synthetic data .....	58
Figure 8-4 - Periodogram for real wind data (left) and synthetic wind data (right).....	60
Figure 8-5 - Wind speed trajectories for three different wind farms .....	61
Figure 8-6 – Wind speed trajectory and corresponding electric power generated for a wind farm .....	61
Figure 8-7 - Periodogram for electric power generation for a wind farm (left) and the total national (right).....	62
Figure 8-8 - Power generation for a wind farm (up), a group of wind farms (middle) and the total for the country (down).....	63
Figure 8-9 - Probability distribution for a wind farm (up), a group of wind farms (middle) and the total for the country (down).....	64
Figure 8-10 - Comparison of turbulent component for wind power generation of a wind farm (black), a group of 12 wind farms (blue) and all the projects modeled (red) .....	65

## RESUMEN

Teniendo en cuenta la creciente necesidad de expansión del sistema eléctrico chileno, la búsqueda de nuevas fuentes de energía se ha transformado en una prioridad nacional para Chile. El recurso eólico puede considerarse como un nicho energético maduro, con tecnología a precio de mercado y una aparente disponibilidad en el territorio nacional. Esta alternativa se presenta como una opción factible de implementar, probablemente con representando un rol importante en el desarrollo futuro de la matriz eléctrica chilena.

Con el objetivo de entender el recurso eólico local, en primer lugar estudia los perfiles eólicos disponibles en la zona norte y centro del país, convirtiéndose en el primer estudio público de este tipo.

Utilizando modelos autorregresivos, mediciones reales, datos satelitales y análisis en el dominio de la frecuencia, es posible generar datos sintéticos de viento que recojan el comportamiento natural del recurso. Estos datos pueden ser utilizados para suplir la falta de información detallada del recurso en lugares como Chile donde no existe gran disponibilidad de datos. Esta investigación presenta un modelo de generación sintética de viento para generar series de viento en localidades donde se ubican potenciales proyectos eólicos pero no existen datos detallados del recurso local. Con esta información se estudia el efecto de agregar generación eólica al sistema eléctrico Chileno, lográndose observar como a mayor número de parques eólicos instalados, la variabilidad se ve reducida y la generación agregada presenta una componente de generación base. Finalmente se calcula el factor de planta eólico agregado nacional

obteniéndose un valor de 29.2% considerando sólo los proyectos con factores de planta mayores a 20%. Estos modelos se convirtieron en la base que se utilizó en la participación de Chile en la COP15.

Palabras claves: Viento, velocidad del viento, energía, autorregresivo, frecuencia, factor de planta, electricidad, Chile

## **ABSTRACT**

Bearing in mind the current and pressing need for an update of the existing Chilean power supply system - which has been remarkably influenced by new requirements - the search for new energy supply sources has become a top priority.

The wind resource, vis-à-vis its associated mature technology features and its apparent availability throughout Chile, comes forward as a feasible option likely to play a more important role in any future national energy generation matrix.

With a view to understanding the local wind resource, this document surveys a sample set of wind profiles available in the northern Chile area, thus becoming the first public survey of this kind.

Using autoregressive models, actual measurements, satellite data and analysis in the frequency domain, it was possible to generate synthetic data of wind including the natural behavior of the resource. These data was used to address the lack of detailed information of the resource in places like Chile where do not exist high data availability.

This research presents a model for synthetic generation of wind to generate series of wind potential locations where wind projects are located but there are no detailed data on local resource. With this information we study the effect of adding wind generation to the Chilean electrical system, observing how as a greater number of wind farms are installed, the variability is reduced and the total generation shows a base component. Finally we calculate the factor of national aggregate wind capacity factor of 29.2% considering only the operating projects and the future projects with a capacity factor

over 20%. Those became the basis of the wind modelling we undertook for Chile's participation in COP15.

Keywords: Wind, wind speed, energy, autoregressive, frequency, capacity factor, electricity, Chile.

## 1. INTRODUCTION

The energy supply issue is now a subject with wide-ranging and urgent implications in the national discussion. Now the uncertainty surrounding the Chilean power supply future and the lessons learnt from past crises have come into play. The past and grim experiences derive mainly from the influence of climate change and - to a greater extent - from the dependency caused by foreign supply fossil fuels. Such factors plus a limited diversification drive are currently reflected in the energy matrix. Stemming from the Argentinean gas supply crisis experienced a few years back, the future overall energy scenario has become a key subject within the political agenda. From this viewpoint, a thorough and proper understanding of future energy supply alternatives is now a matter of crucial importance.

On the other hand the environmental preservation needs, to which all electric systems are becoming subject to, are causing a surge in a series of requirements and restrictions to be met by any system's expansion technologies. The compelling need to produce an energy matrix more environmentally friendly is influencing developing countries such as Chile to pay a growing attention to renewable technologies (both conventional and non-conventional). The aim here is to ensure they reach a more developed status so they can be inserted in future expansion plan<sup>1</sup>. Likewise, the availability of various renewable energy resources within Chile is influencing an upswing of such interest amid key decision-takers.

---

<sup>1</sup> Following Chile's recent incorporation to OECD, there will be more exacting environmental requirements to be observed and met from now onwards.

Wind energy rates as a possible alternative which, while complementing other energy options, could eventually supply a significant fraction of future energy needs. All this while ensuring the national energy matrix still entails operational and expansion criteria based on environmental sustainability.

In this paper we describe the few wind projects developed so far, most of them commissioned at the end of 2009 following the recent regulatory changes. We also provide statistics on the only large scale operational project. Thereafter we include a detailed analysis of eight wind profiles in various areas together with indicators such as the monthly and daily averages plus estimates of potential energy production and capacity factors we conclude that there is an important potential for wind power exploitation in the northern Chile area.

## **2. CURRENT ENERGY SCENARIO AND THE WIND ROLE**

When it comes to pay a closer look at the insertion of a specific type of energy, in this case wind power, the essential requirement is to understand the overall energy scenario within which such technology will be competing. If we are to understand the conditions for this technology to develop, not only must we survey it as a resource, but become fully acquainted with the existing energy matrix and the trends influenced by the current “business as usual” policy. Likewise, it is also important to be conversant with the system areas in which wind power could penetrate and where current projects have been already implemented. In short, it is crucial to achieve a thorough understanding of the climate and geographical configurations of the areas were the surveys are undertaken.

### **2.1. A breakdown of the Chilean energy matrix**

The national power system entails four independent subsystems, namely: The Northern Chile interconnected system (Name in Spanish: Sistema Interconectado del Norte Grande - SING), the Central Chile interconnected system (Name in Spanish: Sistema Interconectado Central - SIC) and the medium-sized systems covering the southernmost Chilean areas of Aysén and Magallanes. Amid these four subsystems, the two main ones are SIC and SING encompassing a 99% of installed capacity and 91% of total generation (Borregaard, 2009)(p. 10). The specific composition of each of the subsystems, particularly the two main ones, is unique.

The SIC system entails a large presence of hydroelectric energy (conventional) with a supplement of thermal systems based on coal and diesel oil. On the other hand, the

SING system is essentially thermal with a negligible presence of other power generation alternatives. Table 2.1 shows the breakdown of the power generation park at April 2009 as specified by the National Energy Commission (name in Spanish: Comisión Nacional de Energía - CNE) in its customary report on installed capacity broken down by each interconnection (2008) and in the nodal prices report for SIC's interconnection at April 2009 (Borregaard, 2009)(p.10)(CNE, 2008, 2009a). A similar breakdown for SING is shown on Table 2.2 as per its nodal prices report and the same capacity report mentioned beforehand (CNE, 2008, 2009b). The installed capacity percentage distribution for both systems can be seen on Figures 1 and 2. It can be noted that the current presence of renewable energy sources is very small and the whole market is dominated by conventional thermal and hydraulic technologies.

Table 2.1 – SIC's installed capacity - April 2009

<b>Technology</b>	<b>Capacity [MW]</b>	<b>% of total capacity</b>
Hydro - Water dam	3,393.40	33.40%
Hydro - Run-of-the-River	1,516.30	14.90%
Diesel oil - TG	1,734.10	17.10%
Diesel oil - CC	1,978.40	19.50%
Diesel oil - CA	549.9	5.40%
Coal	796.2	7.80%
Biomass	172.9	1.70%
Wind	18.2	0.20%
<b>Total</b>	<b>10,159.30</b>	<b>100%</b>

Table 2.2 - SING's installed capacity - April 2009

Technology	Capacity [MW]	% of total capacity
Hydro - Run-of-the-River	12.7	0.4%
Diesel oil - TG	332.9	9.4%
Diesel oil - CC	1,441.2	40.5%
Coal	1,135.8	31.9%
NG CC	632.7	17.8%
Total	3,555.3	100%

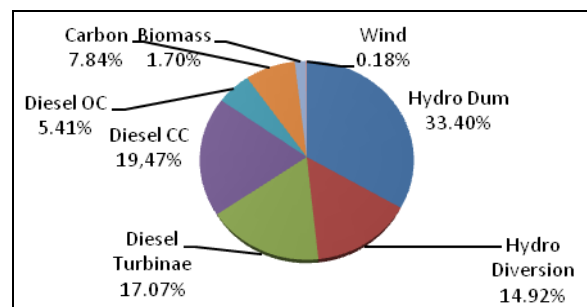


Figure 2-1– Percentage breakdown of SIC's installed capacity – April 2009

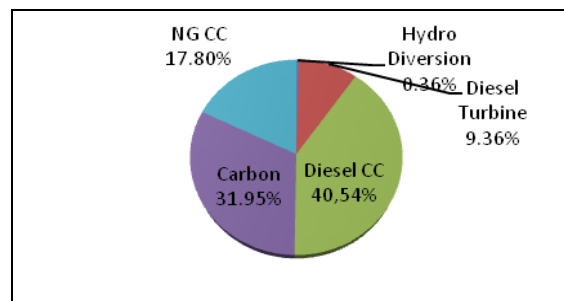


Figure 2-2 – Percentage breakdown of SING's installed capacity

Thanks to the country's geographical features, the prospecting work leading to the installation of onshore wind power units appears to be more feasible as opposed to offshore equivalents. However the abrupt gorges and ravines along most of the northern Chile coastline and the depth of the coastal plateau found elsewhere suggests

that the installation of offshore wind power technology has little or no implementation prospects in most regions. That said, promising prospects stem from the geographical viewpoint in the form of high-altitude mountain ranges, an extensive highland plateau areas throughout most of the Chilean territory. All such areas are rated as with a great potential for onshore wind power generation units.

Figure 2-3 shows the Continental Chile area with indications of its main regional design, together with an indication of the various power systems within and the location of existing main cities.



Figure 2-3 – Continental Chile and her power systems

## 2.2. Chilean projects on wind power

Following the enactment of Chilean Law # 20,257 which makes it legally enforceable for power companies to include a quota of power generation based on non-conventional

renewable energy sources (NCRE), a demand throughout Chile for such energy sources has been created. Thus renewable energies are showing an incipient expansion with a number of projects already approved and others undergoing the official approval formalities. Although Law # 20,257 has a compelling clause asking power companies to partially operate on the basis of renewable energies, the expected real-life effects of this arrangement are not entirely clear yet. Indeed the lack of fulfilment of the NCRE quota requirement calls for the payment of fines that sometimes may result in a reduced direct cost when compared to the equivalent NCRE input. However, it is clear that NCRE options have started their expansion and their contribution to the energy matrix should grow in coming years.

In early 2009 the only wind power generation project with any relevance within SIC was the “Canela” wind farm owned by ENDESA(CNE, 2008). Such wind farm is next to the small Canela settlement and not far from other conurbations known as “Pan de Azúcar” and “Los Vilos” in Coquimbo. Its installed capacity is 18 MW produced by 12 Vesta V82 generators of 1.5 [MW] each and is connected to SIC’s 220 [kV] power line section linking up Pan de Azúcar and Los Vilos. This project came on stream in late 2007 and represents the initial precedent for SIC as far as wind power generation is concerned (SEIA, 2007). However, in late 2009 and early 2010 some significant changes took place. Indeed, since early 2009 a number of wind farms came on stream, chiefly in the Northern Chile area. In addition to “Canela”, we have noticed the commissioning of the wind farms known as “Totoral” (46 MW), “Monte Redondo” (38 MW), “Canela II” (60 MW) - all in Northern Chile’s Region IV plus “Lebu” (2.76 MW) in region VIII and “Alto Baguales” (4.25 MW) in Region XI. The latter farm is

the oldest of its kind in Chile. Several other projects are expected to come on stream in the near future and our group is performing a review of those projects and is involved in the surveys for some of them. Projects under evaluation add up to 2,021 MW.

### **2.3. Wind energy and how it is coping with the SIC demand**

It is also interesting to look into the existing wind power generation specific performance and its supply contribution to the daily peak demand. Based on the CNE historical records we calculated the SIC's average hourly consumption for year 2008 and the relevant hourly average wind power generation for the same year. This was undertaken for each hour interval at the "Canela" wind farm (at the time the only one connected to the SIC system). The demand data considered was only the average readings for work days (in order to identify its contribution to the peak). We noted that the wind power generation peak does not correspond with the hour of maximum demand in a day, thus there was a limited correlation between wind power generation and power demand.

Likewise, the hour of maximum wind power generation was at night time (8 PM) with an annual average value in the region of 7.01 MWh, equivalent to 0.1% of the power contribution generated in the specific hour. The demand peak hour (11 PM) wind power represented a 4.8 MWh contribution, equivalent to 0.08 %.

The foregoing denotes the minimum penetration rate secured by wind power in the Chilean grid. Figure 2-4 shows such performance which, as far as wind power is concerned, indicates an error equivalent to its standard deviation for the period. Figure

2-5 shows the duration graph which relates to the data shown in Figure 2-4, and shows the small contribution of wind power to the overall system generation figure.

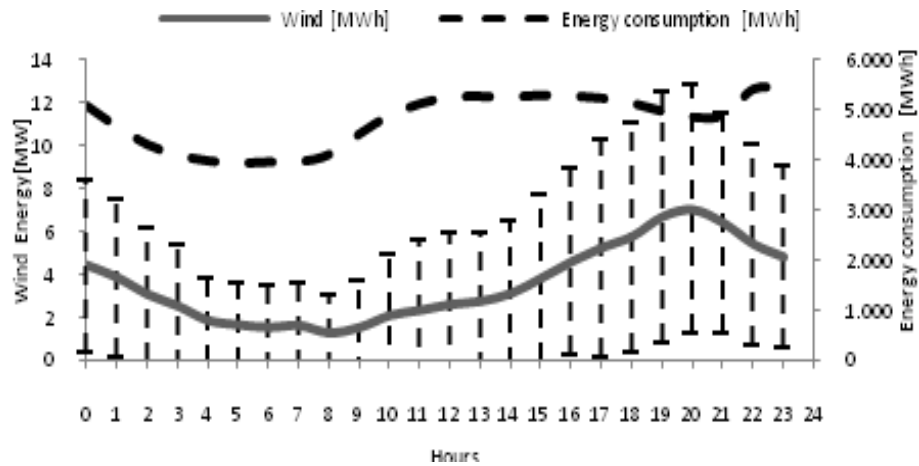


Figure 2-4 – Average annual generation and wind power generation in the SIC grid, year 2008

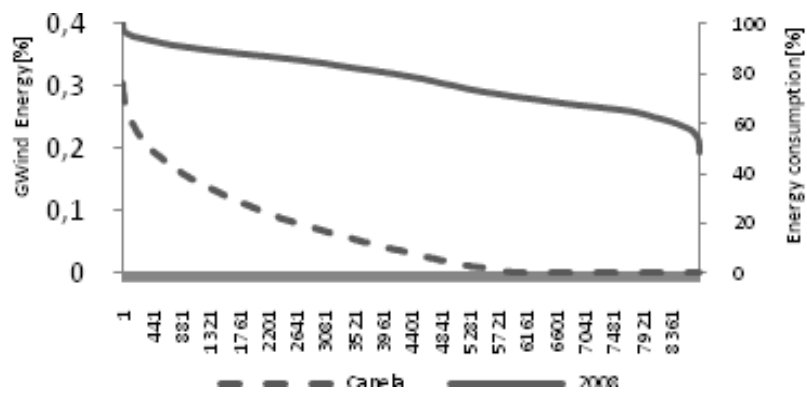


Figure 2-5 - Duration graphs for consumption and wind power generation in the SIC grid.

### **3. MEASUREMENTS AND THE CHILEAN WIND RESOURCE**

Although Chile appears to have a wind power generation potential well worth tackling, the current state of play concerning intellectual capital, public data and a supporting institutional structure is scant. However, the need for a larger development in the renewable energies' area has boosted a number of relevant surveys aimed at a more accurate quantification of the renewable resources yet to be tackled throughout Chile.

In August 2009, the National Energy Commission issued the preliminary version of the survey known as (name in Spanish) "Prospección Eólica en Zonas de las Regiones de Atacama, Coquimbo y el Maule" (Wind Prospection Survey in the Atacama, Coquimbo and Maule Regions) (CNE, 2009d). This survey summarises the public weather station data compilation work done on specific features concerned with all climate and geography factors and which could highlight comparative advantages for a future tackling of wind power prospects.

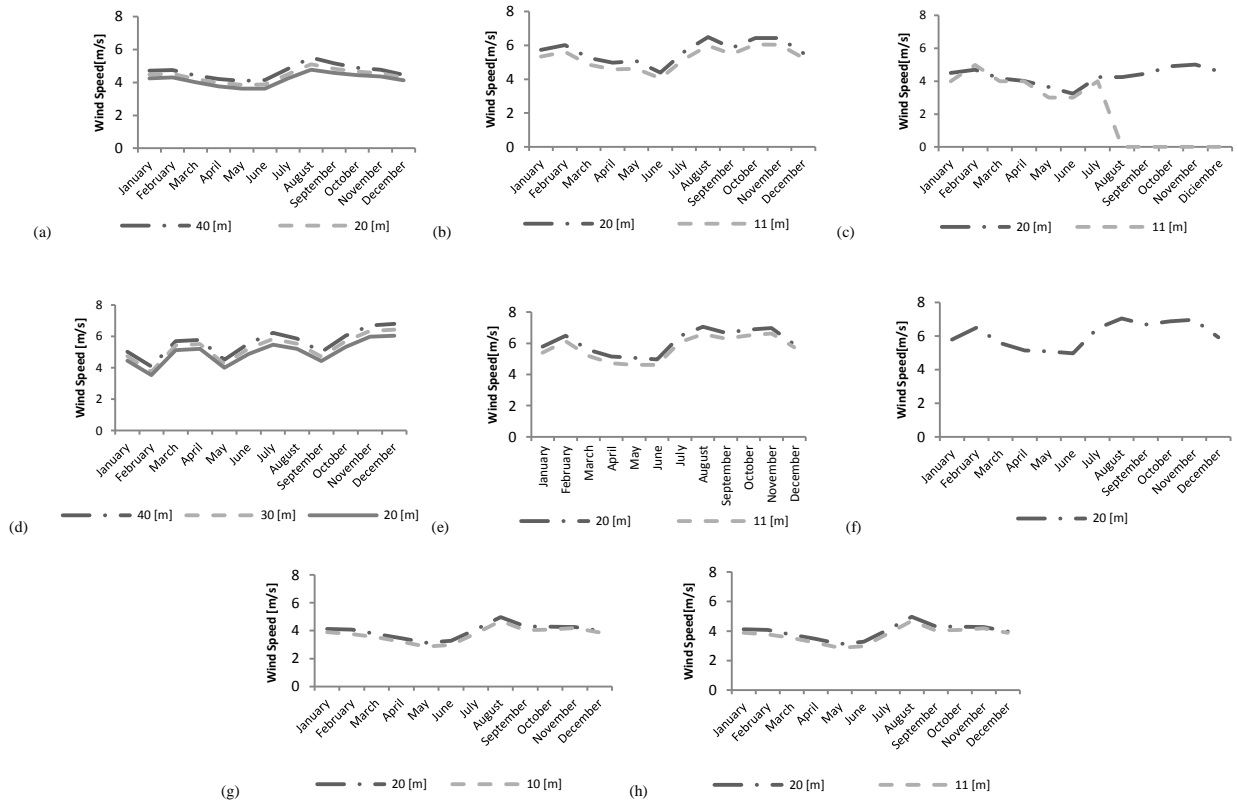


Figure 3-1 – Annual average speeds: Carrizalillo (a), Cebada Costa (b), Cerro JP (c), Faro Carranza (d), Lengua de Vaca (e), Llano de Chocolate (f), Loma del Hueso (g), Los Choros (h)

Within such locations in Atacama, Coquimbo and Maule (CNE, 2009d) (p. 2), there are some coastal zones. It is precisely there where you can note wind profiles generated by the combination of wind flows stemming from the coastal area and other flows generated by thermal effects. The latter are usually associated to the presence of transversal valleys that generate wind flows assisted by a steady sunlight presence

(CNE, 2009d) (p. 6). Due to a recurrence of some climate and geographical features alongside the Chilean national territory, it makes sense to expect the performance surveyed at the measurement stations to replicate elsewhere.

It follows that the survey analysis could become a significant tool for the initial estimate of the wind power generation potential currently available throughout Chile.

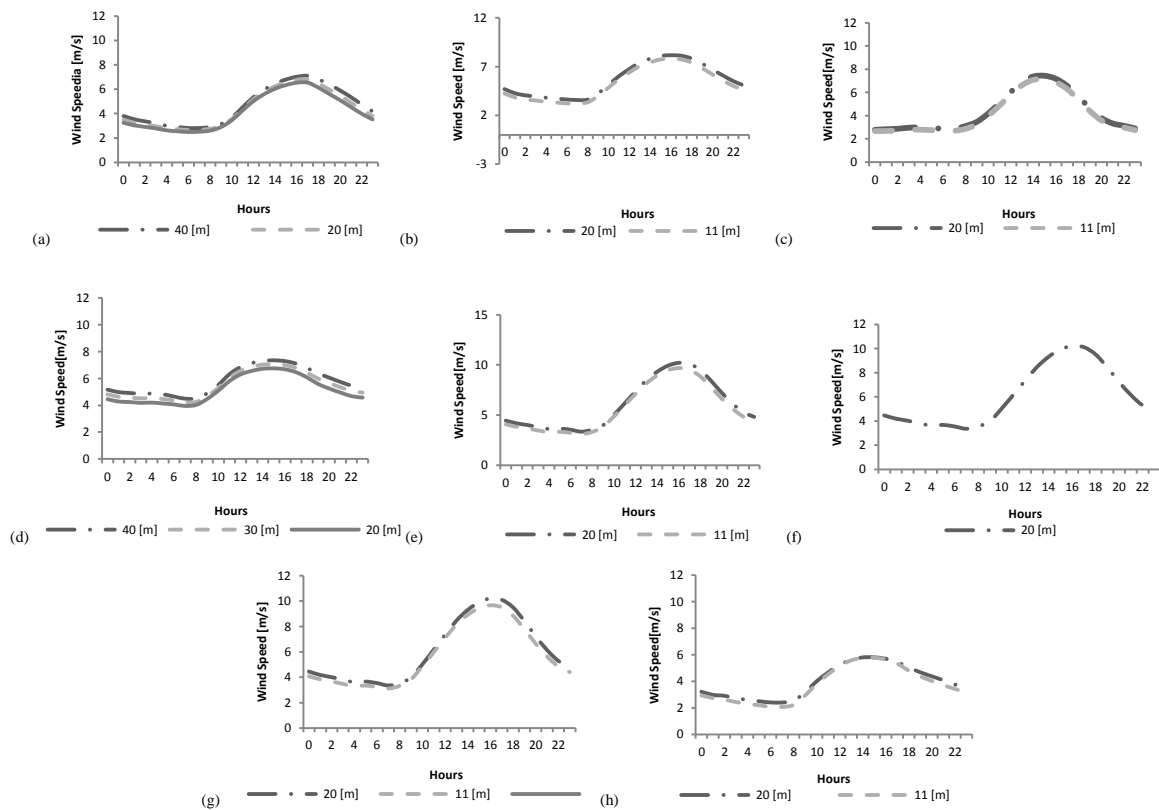


Figure 3-2 – Daily average speeds: Carrizalillo (a), Cebada Costa (b), Cerro JP (c), Faro Carranza (d), Lengua de Vaca (e), Llano de Chocolate (f), Loma del Hueso (g), Los Choros (h)

### **3.1. Wind zones and measurements**

Due to the foregoing the CNE, together with the German Technical Cooperation Agency (better known for its GTZ acronym), the United Nations Development Programme (UNDP) and the co-financing support provided by the Global Environmental Facility (GEF), is currently implementing a wind profiling pattern drive in the zones showing the foregoing features (CNE, 2009d) (p. 2). On the basis of this initiative, a number of locations were selected for specific surveys on the wind profiles for the specific areas of interest. The locations selected in the first stage of the campaign were:

- Los Choros, Llano – Chocolate (Atacama Region, Northern Chile)
- Quebrada del Teniente (Coquimbo Region, Central North Chile)
- Chanco (Maule Region, Central South Chile)

This specific monitoring drive entails also the information compiled by a monitoring station at the “Lengua de Vaca” zone. Due to the fact that the Geophysics Department of the University of Chile has operated a meteorological station since the early 90s (CNE, 2009d) (p. 3), such data is considered for reference purposes only.

Stemming from the above, and in a first stage, a total of eight monitoring stations are being considered for the Northern Chile area. Such stations are “Loma del Hueso”, “Llano de Chocolate”, “Carrizalillo”, “Punta Los Choros”, “Punta Lengua de Vaca”, “Cerro Juan Pérez”, “La Cebada Costa” and “Faro Carranza”. The readings were taken in period 2006 - 2008, although the stations with the single exception of “Faro Carranza”, cover only part of year 2006 since they were installed and commissioned

halfway through that year. We must also bear in mind that five of the stations are fitted with anemometers at 11 and 20 metres high, whereas Carrizalillo's equivalent wind measuring gauges are placed at 11, 20 and 40 metres and Faro Carranza's own are at 20, 30 and 40 metres (CNE, 2009d) (p. 3). Regrettably there are no readings taken at the hub altitude of large scale generators. Figure 3-3 shows the location of each reading point together with readings for the nearby city of Coquimbo plus those for "Canela" and "Totoral" wind farms Table 3.1 summarises the main features of the various monitoring stations considered in the survey. It shows the name of the station, its geographical position, its above-sea-level altitude, its sampling start and completion dates, the data integration interval length<sup>2</sup> and a description of each specific anemometer with its altitude details.

### **3.2. Summary of the Wind Survey**

Based on the wind prospecting report findings in Atacama, Coquimbo and Maule (CNE, 2009d) and the additional data in the form of a public document placed on the website containing such report, the authors of this paper worked further on the data and produced their own wind resource evaluation which hitherto had not been available in Chile.

When analyzing the wind resource, its profile calculations were taken into account as a summary of the average data for each hour of the day and month of the year. Polar graphs such as the wind rose type were also considered, chiefly for identifying the

---

<sup>2</sup> En Cebada Costa no se consta con datos entre el 05-11-2006 y el 21-12-2006.

average wind direction and its energy density broken into each direction, the wind's vertical shearing profile and its empiric and adjusted probability values' distribution. Whenever possible, the wind power density values were also calculated, with a view to securing a resource classification based on a standard scale.

Last but not least, it includes the power generation calculation with the use of a 1,525 kW REpower MD77 wind turbine parameters. This inclusion was aimed at providing a notion of the energy and capacity factor associated to the wind resource.

Table 3.1– Summary table of the main features at each measuring position

Nombre estación	Latitud	Longitud	E.S.N.M. [m]	Inicio muestreo	Fin de muestreo	Δts [min]	Anemómetros/alturas [m]
Carrizalillo	29° 2'29.00"S	71°23'45.00"O	161	13-07-2006	12-03-2008	10	Thies a 40 [m], 20 [m] y 10 [m]
Cebada Costa	31° 01'53.94" S	71° 37'42.84"O	265	03-06-2006	12-01-2008	10	NRG a 20 [m] y 11 [m]
Cerro Juan Pérez	30°56'50.46"S	71°33'48.84"O	606	13-06-2006	12-01-2008	10	NRG a 20 [m] y 11 [m]
Faro Carranza	35°32'32.30"S	72°35'20.90"O	21	29-01-2006	08-06-2007	10	Thies a 40 [m], 30 [m] y 20 [m]
Lengua de Vaca	30°14'51.18"S	71°37'43.38"O	53	26-09-2006	21-07-2008	10	NRG a 20 [m] y 11 [m]
Llano de Chocolate	28°57'50.70"S	71°14'34.08"O	360	02-06-2006	10-01-2008	10	NRG a 20 [m] y 11 [m]
Loma del Hueso	28°54'28.38"S	71°27'1.44"O	21	29-01-2006	08-06-2007	10	NRG a 20 [m] y 11 [m]
Punta los Choros	29°14'17.58"S	71°25'48.72"O	16	03-06-2006	11-01-2008	10	NRG a 20 [m] y 11 [m]

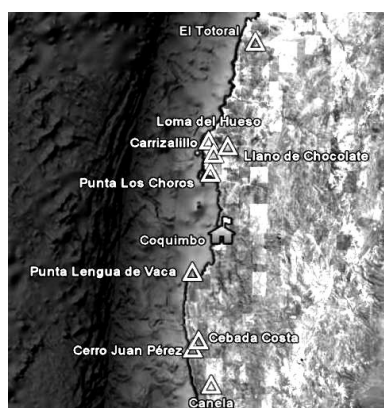


Figure 3-3 – Location of the measurement sites and associated milestones

### **3.3. Time frame of measurement**

The measuring stations considered in this survey produced eight data sets sampled from mid 2006 through to early 2008. For this specific survey stage we used the whole 2007 data for making all our calculations and left out all the other data. There were two exceptions whereby we used the 2006 and 2007<sup>3</sup> data, chiefly for having a full year's data and thus sparing ourselves the risk of any seasonal over estimations.

Figure 3-3 shows the location of each measurement point together with details referred to Coquimbo plus the already operational “Canela” wind farm and “Totoral”.

### **3.4. The wind Average monthly profile**

The wind average monthly profile allows for the identification of its seasonal and monthly variations coupled with the data of the wind peaks and troughs for the zone concerned. Due to the limited sampling scope, we readily accept that such cannot be regarded as representative enough. Ideally, we should be in a position to produce a data set extending over a number of years.

As stated in

Figure 3-1 we show the monthly profile for the readings undertaken at the sundry locations and at different heights. As far as the “Carrizalillo” and “Faro Carranza” monitoring stations is concerned, the readings were taken at three different heights,

---

<sup>3</sup> The locations of Cerro Juan Pérez, whose data calculations entailed data readings collected in period 3 June 2006 and 3 de June 2007 and Faro Carranza whose data readings' period ranged from 29 January 2006 to 29 January 2007.

thus it was feasible to produce a more detailed and comprehensive profile of the wind resource. To the foregoing we can add the already available pressure and temperature readings that catered for a calculation of the associated power density for such two measuring locations.

In

Figure 3-1 (a) we show the monthly average profile for year 2007 recorded at the “Carrizalillo” monitoring station. A clear cut performance can be noticed from a warm weather type of wind profile that concentrates its highest average readings in the early spring period. On the other hand, the lowest average readings were noted in the winter period. This performance is reported in almost all other measuring stations. Faro Carranza shows the slowest speed in February. As regards maximum speeds, they are reported in the August – December period.

Table 3.2 – Monthly maximum and minimum wind speed readings at 61.5 m.

Location	Minimum	Maximum [m/s]	Average	Stand. Var. [m/s]
	[m/s]		[m/s]	
<b>Carrizalillo</b>	4.21/MAY	5.61/AUG	4.8	2.59
<b>Cebada Costa</b>	5.00/JUN	7.4/AUG	6.46	4.12
<b>Cerro JP</b>	5.52/MAY	7.98/DEC	5.77	3.76
<b>Faro Carranza</b>	4.95/MAY	7.47/DEC	6.34	3.75
<b>Lengua de Vaca</b>	5.58/JUN	7.94/AUG	6.87	4.49
<b>Llano chocolate*</b>	4.97/JUN	6.88/OCT	6.09	3.98
<b>Loma del Hueso</b>	6.66/MAY	8.95/AUG	7.76	3.71
<b>Los Choros</b>	3.46/MAY	5.58/ AUG	4.46	2.57

Table 3.3 – Annual statistical data for the specific location readings

Height/Statistical	Average [m/s]	Stad. Var. [m/s]
<b>Carrizalillo</b>		
40 [m]	4.66	2.48
20 [m]	4.4	2.35
11 [m]	4.18	2.25
<b>Cebada Costa</b>		
20 [m]	5.65	3.56
11 [m]	5.26	3.40
<b>Cerro JP</b>		
20 [m]	4.44	2.92
11 [m]	4.23	2.66
<b>Faro Carranza</b>		
40 [m]	5.79	3.42
30 [m]	5.47	3.24
20 [m]	5.15	3.06
<b>Lengua de Vaca</b>		
20 [m]	6.09	3.98
11 [m]	5.71	3.73
<b>Llano de Chocolate</b>		
20 [m]*	6.09	3.98
<b>Loma del Hueso</b>		
20 [m]	6.08	2.86
11 [m]	5.32	2.6
<b>Los Choros</b>		
20 [m]	3.98	2.22
11 [m]	3.74	2.24

The specific data concerning the maximum and minimum average readings for each measurement site together with details of the month when such reading was recorded is shown in Table 3.2. This information is considered for the maximum height measurements available in each cases considered. This information is referenced at 61.5 m high. The exception is the “Llano de Chocolate” station where there is only one reading. Here we could not obtain the wind speed at 61.5 m high and we merely opted for keeping the original value at 20 m high. In

Table 3.3 we show the average values and the standard variations of wind speeds at different altitudes. Based on the graph data the locations with the best wind power exploitation potential are “Loma del Hueso”, “Llano de Chocolate”, “Lengua de Vaca”, “Faro Carranza” and “Cebada Costa”.

### **3.5. The wind average daily profile**

The daily profile represents the average wind performance during the day, indicating the recording time for the highest and lowest speeds. This is useful data used in a subsequent comparison with demand whenever we can work out to what degree is wind present or otherwise at peak demand times. Figure 3-2 shows the average hourly profile for the locations included in the survey and where it is plain to see the predominance of a daily regime with a peak value in mid-afternoon and a concentration in the highest wind speed hours at around 4 p.m. with variations shown between 3 and 5 p.m. as appropriate.

As regards the minimum speed readings it is plain to see that all locations included in the survey but those referred to the “Cerro Juan Pérez” station shown in Figure 3-2(c), the minimum wind speed is at around 7 and 8 a.m. whereas in Figure 3-2(c) is at 00:00 hrs. The data on the minimum and maximum wind speeds for the areas of interest plus indications of the occurrence time can be seen in Table 3.4. The data corresponds to the escalated samplings at 61.5 m.

Table 3.4 – Daily maximum and minimum wind speed readings in the various locations included in the survey

Location	Minimum [m/s]	Maximum [m/s]
Carrizalillo	2.89/6 hrs	7.43/17 hrs
Cebada Costa	4.04/7 hrs	9.47/ 16 hrs
Cerro JP	3.73/0 hrs	9.96/15 hrs
Faro Carranza	4.89/7 hrs	8.21/15 hrs
Lengua de Vaca	3.77/7 hrs	11.58/16 hrs
Llano chocolate*	3.36/7 hrs	10.11/17 hrs
Loma del Hueso	5.22/7 hrs	10.45/16 hrs
Los Choros	2.59/7 hrs	6.72/15 hrs

### 3.6. Wind rose for the power frequency and density

The wind rose is a polar graph that initially compiles the frequency data associated to each of the possible wind directions distributed over 360°. This graph is useful for identifying the direction trend showed by the wind flows. However, this graph can be produced for other relevant variables and then associate its data to the wind flow directions. In Figure 3-5 we can see the wind rose graph for the wind profile directions in each of the measurement points. It can be seen that all the wind profiles show a preferential SW direction, with the wind sampled at the “Cerro Juan Pérez” station being more focused onto the West.

As per the ideal gas equation:

$$P_r = \rho \frac{R}{M} T \quad (3.1)$$

Pr: Atmospheric pressure [kPa]

$\rho$  : Air density [kg/m<sup>3</sup>]

R: The universal gas constant factor equivalent to 8.314472 [m<sup>3</sup>kPaK<sup>-1</sup>kmol<sup>-1</sup>]

M: Gas molar mass [kg/kmol]

T: Temperature [k]

If we consider an air molar mass equal to 28.9664 [kg/kmol] and with the known temperature and pressure data stemming from the previous readings, we can get the air density data for each of the samplings considered. Once the air density data is to hand, it is feasible to work out the power density available in the surveyed wind profile. For this we have considered the power (P) associated to the wind speed profile as proportionate to the cube of the wind speed (v) as shown in the following equation:

$$P = \frac{1}{2} \rho v^3 \quad (3.2)$$

Once the air density and wind speed are known, it becomes feasible to obtain the power density expressed in [W/m<sup>2</sup>]. Thereafter, and considering the reading interval for each sampling, it is feasible to obtain the energy density associated to the surveyed wind flow expressed in [Wh/m<sup>2</sup>]. In this publication we have considered 10 minutes intervals.

In Figure 3-7 we show the wind rose profile for the energy density associated to the sampled data taken at “Carrizalillo” for a height of 40 m. As expected, the energy

content of the wind corresponds to the most common direction flows. Due to their relationship with the speed cube, small variations in the latter produce significant variations in the energy obtained from the wind. In turn this explains why the energy density graph points towards the same direction than the frequency, albeit it works out somewhat narrower. It is important to highlight the correspondence between the most common wind flow direction and the energy density; with the latter follows the same wind trend as such. However, in the case of Figure 3-7(b), it shows another additional component. In Figure 3-5(d) it can be seen that there are wind components in the same directions noted in Figure 3-7(b).

### **3.7. Vertical wind shear profile**

The vertical wind shear profile is a graph representing the relevant heights for different speeds and shows also how the speeds evolve in relation to the height from the ground level. This evolution is exponential due to the wind performance in respect of the ground contour. Whenever there is a need to calculate the vertical wind shear profile, two different estimation methods can be used. One of them is the power law and the other is the logarithmic profile. Both provide a very similar vertical wind shear profile description. However, for this specific analysis and calculation of such profile we will consider only the power law. The power law assumes the wind speed in relation to the height from the ground changes as per the following expression:

$$v(z) = \beta \cdot z^{\alpha} \quad (3.3)$$

Where:

$z(v)$ : Height from ground level  $z$  [m] for a wind speed [m/s] at such height

$\beta$ : Model constant factor

$\alpha$ : Power law exponent

If the average wind speed for two or more heights over the ground level is already known, then it will be feasible to adjust a curve using the foregoing equation with a view to estimating the power law parameters  $\alpha$  and  $\beta$ . By knowing such exponent ( $\alpha$ ) and the wind speed at some height  $z_1$ , it is possible to use the power law to calculate the wind speed at another height  $z_2$  by resorting to the following formula.

$$\frac{v(z_2)}{v(z_1)} = \left(\frac{z_2}{z_1}\right)^\alpha \quad (3.4)$$

In Table 3.5 we show the parameters which were estimated via an exponential estimation for the various locations included in the survey.

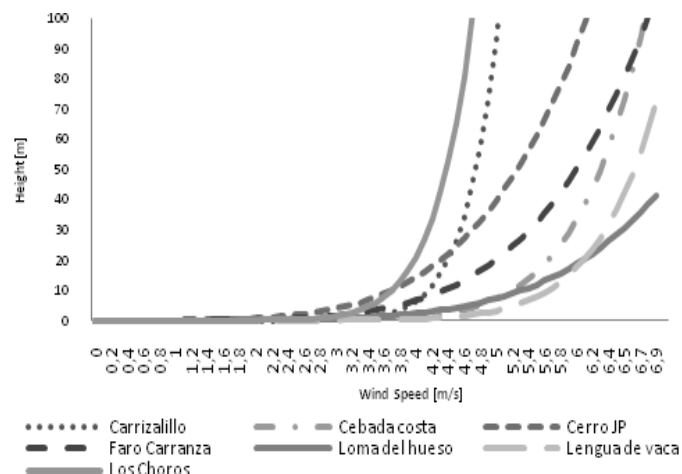


Figure 3-4 - Shearing profile for each location

Table 3.5 – Parameters for the shearing profile in each location

Location	$\alpha$	$\beta$
Carrizalillo	0.083	3.433
Cebada Costa	0.120	3.948
Cerro JP	0.219	2.230
Faro Carranza	0.199	2.750
Lengua de Vaca	0.108	4.410
Loma del Hueso	0.193	3.414
Los Choros	0.104	2.914

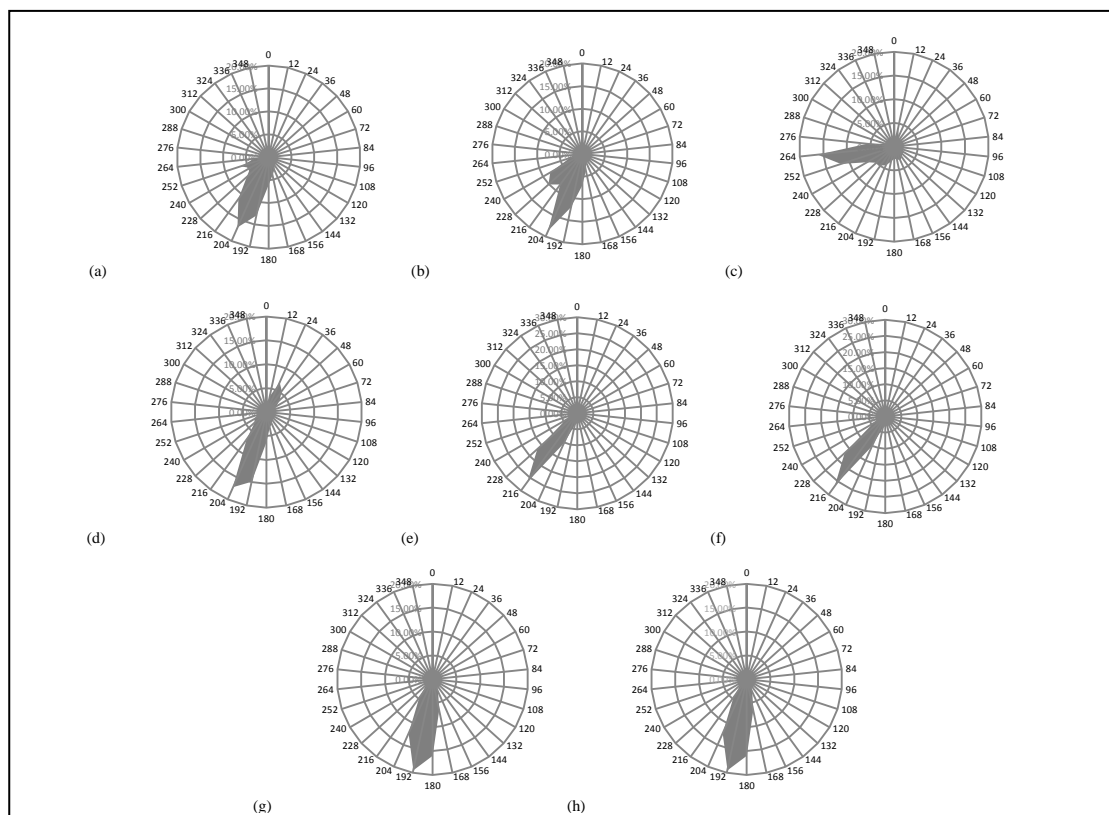


Figure 3-5 – Prevalent wind direction during 2007: Carrizalillo (a), Cebada Costa (b), Cerro JP (c), Faro Carranza (d), Lengua de Vaca (e), Llano de Chocolate (f), Loma del Hueso (g), Los Choros (h)

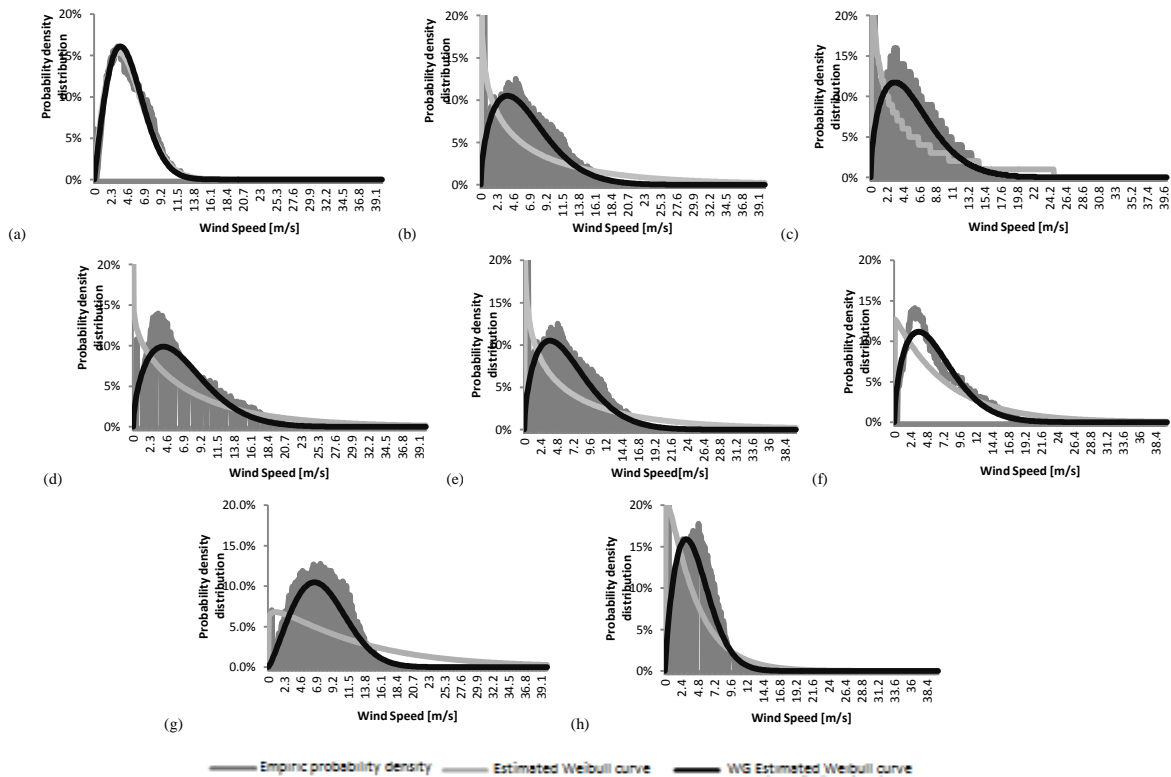


Figure 3-6 – Wind speed frequency with fitted Weibull distribution in all station at 61.5 m for year 2007:: Carrizalillo (a), Cebada Costa (b), Cerro JP (c), Faro Carranza (d), Lengua de Vaca (e), Llano de Chocolate (f), Loma del Hueso (g), Los Choros (h)

Likewise, Figure 3-4 shows the shearing profile for the sampled data at the various locations during the years quoted beforehand. It can be noted that on average, at 80 m. high the wind speed is in excess of 5 [m/s], with an indication that at the altitudes where the wind mills usually operate, the average wind speed is over such value. The

only exceptions are the stations at “Carrizalillo” and “Los Choros” where, as anticipated by the foregoing data, you can expect a low speed profile.

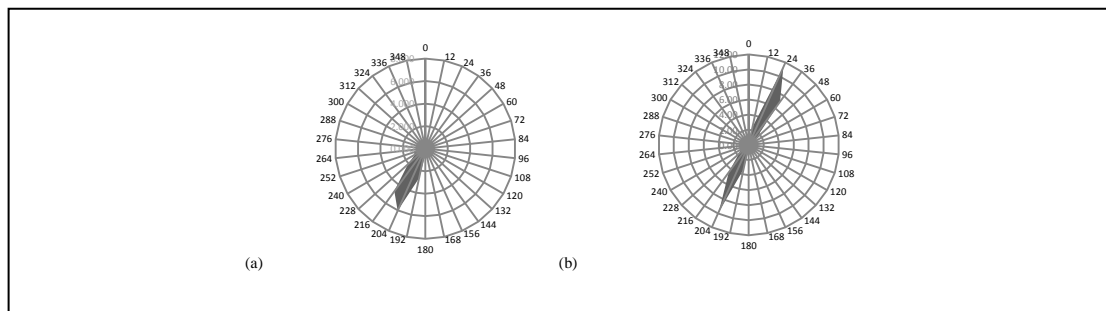


Figure 3-7 – Wind rose for energy density: Carrizalillo y Faro Carranza:  
Carrizalillo (a), Faro Carranza (b)

### 3.8. Empiric and adjusted distribution of Weibull’s statistical resource probability

The probability distribution for the speeds within a wind field shows the likelihood of certain speed ranges during a period of time. The probability distribution can be empirically calculated by classifying the sampled data and thereafter, based on such data, adjust and find the parameters of a known probability distribution. The probability distribution that usually adjusts better to the speed data is the Weibull distribution.

When applying the maximum likelihood estimation method of the measurements undertaken we get the Weibull parameters shown in Table 3.6. Such information is complemented by empiric an estimated graphs showing the probability distribution functions shown in Figure 3-6 for the same measurements. Likewise, we show the Weibull parameters obtained via the special data treatment as worked out with the

assistance of the Windographer software package ( $\alpha^*$  y  $\beta^*$ ) which mitigates some of the problems associated to measurements (Inc, 2010). The graphs shown correspond to the measurements taken on each location and escalated to 61.5 [m]<sup>4</sup>. In the case of various readings taken at different heights, such readings were escalated to the latter height and then averaged.

Location	$\alpha$	B	$\alpha^*$	$\beta^*$
<b>Carrizalillo</b>	1.66	5.22	1.95	5.42
<b>Cebada Costa</b>	0.94	6.55	1.57	7.19
<b>Cerro JP</b>	0.94	4.3	1.55	6.41
<b>Faro Carranza</b>	1.48	6.69	1.77	7.14
<b>Lengua de Vaca</b>	1.03	7.34	1.59	7.68
<b>Llano chocolate</b>	1.03	7.34	1.57	6.76
<b>Loma del Hueso</b>	1.18	3.58	2.2	8.74
<b>Los Choros</b>	1.18	3.58	1.76	5

Table 3.6 – Weibull parameters for the carried out measurements<sup>5</sup>

As regards the cases shown in Figure 3-6 (a) and Figure 3-6 (d) the adjusted distribution to the raw data fits in very well onto the empiric distribution, thus duly representing the occurrence probability of a given wind speed for the profile in question. In all other cases, with special emphasis in Figure 3-6 (a), Figure 3-6 (g) and Figure 3-6 (h), a discrepancy emerges between the empirical and adjusted distributions with the raw data, chiefly due to the existence of a low speed component combined with a high occurrence frequency. Such discrepancy contributes to a poorer adjustment

---

<sup>4</sup> This height was used since it corresponds to the nominal height of the RePower MD77 generator used in subsequent sections for modelling the associated power generation associated to such wind flows.

because it is not properly modeled via the Weibull distribution. The cause of this component is not clear, but it can be attributed to the poor condition of the wind meters used or to some technical problems encountered during the reading stage. However, after a thorough data analysis, we cannot rule out that the measurements correspond to the specific area's natural wind performance, which also points towards the prevalence of protracted still air periods in those areas. For this reason, we included the Weibull distribution worked out with the Windographer software package and its suitable tools for data survey, estimation and filtering. Such tools assisted us in producing much better estimates (Inc, 2010). These new estimates are much better adjusted to the empirical distribution form and exclude part of the low speed component effect mentioned above.

#### **4. AVAILABLE ENERGY AT THE SURVEYED AREAS**

An important objective of this survey is the implementation of an analysis focused on the power likely to be generated from the wind blowing through the various measuring stations included in this survey. A capacity factor is a key parameter for wind power economics and our renewable energy models for COP 15 need estimations of those.

It becomes necessary to select the type of wind turbine and use its power curve with a view to identifying the power series associated to the wind speed series available at each of the stations. In this way we selected a standard 1.525 kW REpower MD77

---

<sup>5</sup> The parameters marked (\*) represent the values calculated using the WindoGrapher software package.

generator, operating at an 61.5 [m] hub height and fitted with vanes whose diameter is 77 [m] (inc., 2009).

We developed a polynomial estimation of the generation curve for this specific generator. The graph representation of such equation is in Figure 4-1. There is an initial period with a speed range extending from zero to 3.5 [m/s] where the output power starts to be described by the estimated polynomial curve until it reaches a value of 11.1 [m/s]. Here the output power reaches its maximum and nominal value equivalent to 1,525 kW and remains steady until the wind speed gets to 25 [m/s] - the so-called cut-off speed. Due to safety considerations, the power output and wind mill rotor are stopped for all higher wind speeds' spectrum.

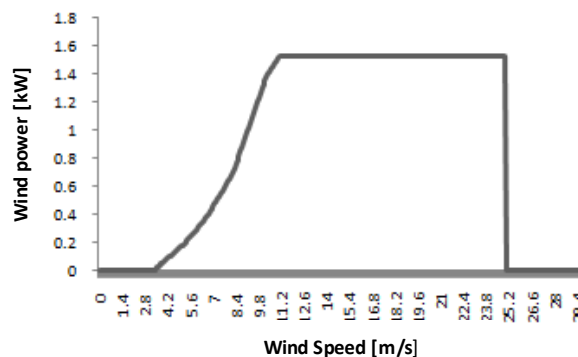


Figure 4-1 – Power curve of the REPower MD77 generator with a 1,525 kW rating

With this function the calculation of power from a wind generator became feasible for each of the wind profiles previously analysed.

The foregoing tallies with the data in Figure 4-2, where it shows the capacity factor calculated on the basis of the previous energy estimates with the REpower MD77

generator. If we assume a maximum operation of 8,760 hours, the maximum theoretical capacity factor is:

$$\text{Capacity Factor} = \frac{\text{Energy [MWh]}}{1,525 \cdot 8760} \quad (4.1)$$

Figure 4-2 shows the capacity factors calculated with this expression for each of the locations concerned. It is clear that there are locations with very high capacity factors as opposed to other locations. “Loma del Hueso” (44.8%), “Lengua de Vaca” (36%), “Cebada Costa” (34.7%), “Faro Carranza” (31.8%) and “Llano de Chocolate” (30.5) have a very high capacity factor, exceeding by far the equivalent 19.4% rating for “Canela” in year 2008. Likewise, the “Cerro Juan Pérez” location shows a very acceptable 27.4% capacity factor. The locations with the lowest capacity factors are “Carrizalillo” (17.2%) and “Los Choros” (14.9%). The foregoing reaffirms the presence of high wind profiles in some locations for the sampling period concerned. If we have to draw out a conclusion or carry out more decisive inferences, then comes along the requirement for the production of longer reading series.

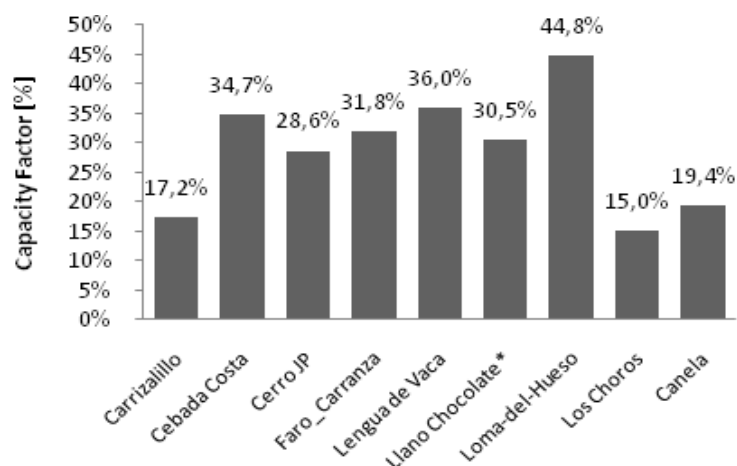


Figure 4-2 - The capacity factors for various data reading locations as opposed to the readings at the “Canela” wind farm.

The foregoing theoretical calculations do not consider the losses associated to the shadow effect and availability. This is simply because our intention at this stage is to provide an approximate notion of the resource and not specific measurements associated to a particular project structure<sup>6</sup>. An economic evaluation calls for the use of more background details and specific conditions associated to the project and the technologies to be considered alike. The above losses would slightly reduce these factors.

---

<sup>6</sup> Under these standards, the Canela’s real capacity factor should be slightly increased if we are to both control these effects and calculate the theoretical capacity factor.

## **5. SEASONAL BEHAVIOR OF WIND RESOURCE**

The wind energy comes mainly from the sun. The movement of air masses that cause the wind is due to both, global and regional components, as local components such as temperature gradients and the local topography, comprising periodic patterns in the wind behavior. The observation shows that there are seasons when the wind blows harder than others and times of day when usually it's seen a higher wind speed. This trend is repeated over time, so it is a seasonal or periodic behavior. The main components observed in the seasonal behavior of the wind speed are the synoptic component, the day – night component and the turbulent component.

### **5.1. Main components in the Wind Speed Behaviour**

The synoptic component refers to weather patterns that affect the wind on a local level. These patterns can affect wind speed for periods from two to ten days with a typical average of four to five days. The variation in the duration of the effect of weather patterns on the wind is variable and highly dependent on local conditions and season (Burton, Sharpe, Jenkins, & Bossanyi, 2001).

The day-night component corresponds mainly to the effect on wind behavior that the sun and therefore temperature differences have. Typically there are periodic components of 24 and 12 hours. This is consistent with casual observation of the wind, where it is expected that the wind tends to blow in a similar way at the same time each day and there is a change in wind speed between day and night (Archer & Jacobson, 2005; Burton, et al., 2001; Watts & Jara, 2011). Figure 5-1 shows the daily profiles for

three sites located in coastal northern Chile, where the trend day – night is observed (Watts & Jara, 2011).

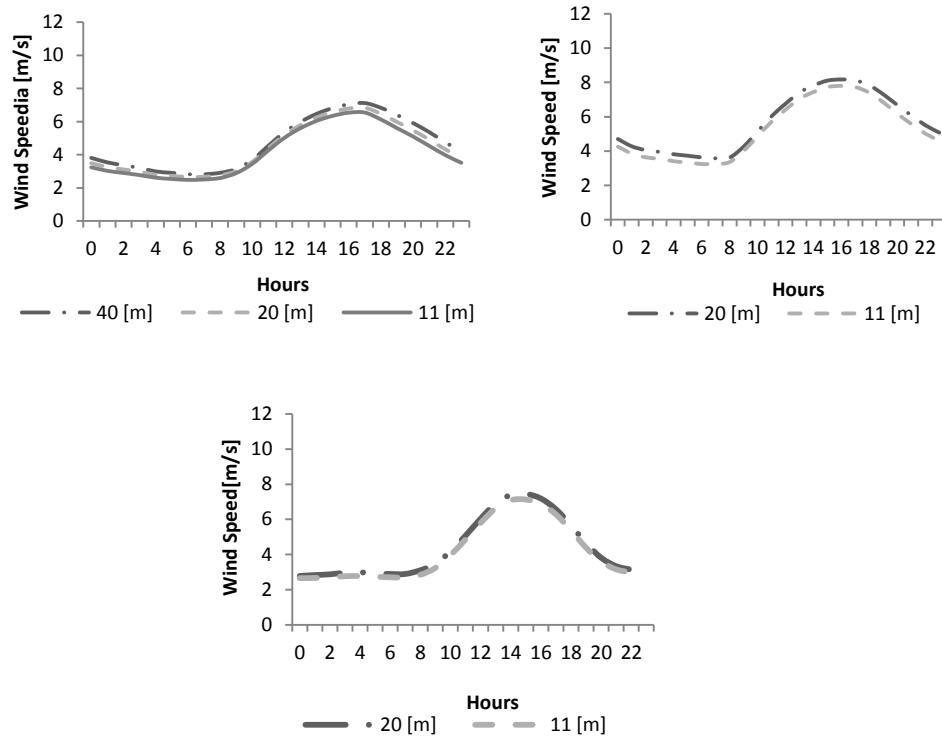


Figure 5-1- Average monthly profile for locations: Carrizalillo (izq.), Cebada Costa (cen.), Cerro JP (der.)

The turbulent component represents rapid fluctuations that wind speed has on a time scale among the few seconds until one or two minutes. The effect of the turbulent component is highly dependent on surface roughness where the wind is blowing and local thermal conditions (Burton, et al., 2001). These variations are responsible for the known bursts of power generated by wind farms connected to power systems, which

can generate significant problems of frequency and voltage regulation in the network, affecting the reliability of systems.

## **5.2. Frequency spectrum for the wind resource: Kolmogorov spectrum**

Wind speed can be studied using a Fourier analysis. The power spectrum in the frequency domain can be calculated for wind data. It is possible to observe the most important components of the Fourier spectrum, which represent the periodic or seasonal component present in the wind.

In a frequency analysis, Kennedy & Roger (2003) observing the frequency spectrum of the hourly average wind speed for 16 years, estimate the most important periodic components. These correspond to components with a period of 5.4 days, 24 hours and 12 hours (Kennedy & Rogers, 2003). Figure 5-2 shows the Fourier spectrum for hourly data of wind speed in Chile for a year of measurement, which shows that the most important representative periodic components has a period of 24 hours, 12 hours and 8 hours.

Fourier analysis can be extended to the electricity generated by a wind farm. As expected, as seen in the frequency domain, there is a correlation between electricity generation and periodic components of the wind. Katzenstein, Fertig and Apt (2010) estimate that the most important periodic components in wind generation correspond to periods of 5 days, 24 hours, 12 hours and 1 hour (Katzenstein, Fertig, & Apt, 2010). It is also important to note that the turbulent components of the frequency spectrum of wind generation can be approximated by a linear function equal to  $f^{-\alpha}$ , a function known as the Kolmogorov spectrum. The Kolmogorov spectrum gains relevance when

analyzing the content of the turbulent components when adding uncorrelated wind farms because of the distances between them (Apt, 2007).

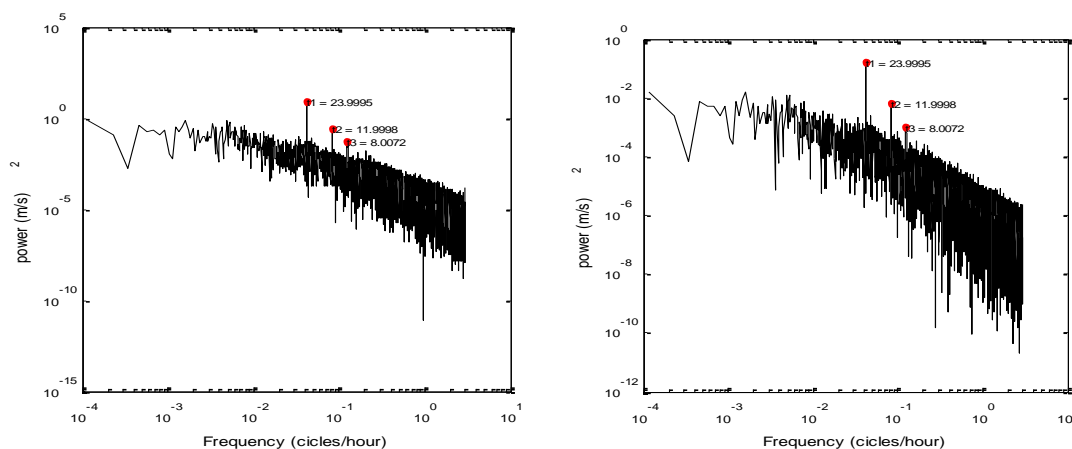


Figure 5-2 – Periodogram for average wind speed for a year (left) and for power generation of one wind farm (Right)

## 6. WIND RESOURCE MODELLING USING AUTOREGRESSIVE MODELS

The wind resource has historically been modeled using the Weibull distribution. This has allowed evaluating wind generation projects. However, this approach does not recognize the temporary nature of wind speed and the existence of seasonal components. For this reason it is necessary to use other models considering these elements, especially in a scenario of increasing penetration of wind generation where their impacts on power system are far from negligible.

### 6.1. Typical modelling in wind resource evaluation: Weibull distribution

The Weibull distribution (two parameters) is a habitual probabilistic approximation to model the behavior of wind speed. The value of these parameters depend of the

climatic and geographical conditions of the specific area (Novoa & Jin, 2011). This distribution has been used many times in different studies to describe the probabilistic behavior of the wind. Watts and Jara described the Weibull distributions for 8 localities in northern Chile obtaining values for the parameter  $\alpha$  between 1.55 and 2.2 and for the parameter  $\beta$  between 5.0 and 8.74 for data sets of one year (Watts & Jara, 2011). Similar estimations have been made by Vallée where this distribution is used to model the wind resource for three European regions (Vallee, Lobry, & Deblecker, 2007) and Spahic, estimating Weibull distributions for the wind resource in the North Sea in Europe (Spahic et al., 2009). The probability density functions and cumulative probability of the Weibull distribution is observed in equations and (6.2).

$$f(v, \alpha, \beta) = \frac{\alpha}{\beta} \cdot \left(\frac{v}{\beta}\right)^{\alpha-1} \cdot \exp\left\{-\left(\frac{v}{\beta}\right)^\alpha\right\} \quad (6.1)$$

$$F(v, \alpha, \beta) = 1 - \exp\left\{-\left(\frac{v}{\beta}\right)^\alpha\right\} \quad (6.2)$$

Although the Weibull distribution can be used to randomly generate values of wind speed and uses this information in wind prospecting studies to evaluate generation projects, this approach does not consider the temporal correlation of wind speed presents. Then, it is not possible to include with this type of analysis, seasonal components and trends, so it requires the use a more complex approaches such as using autoregressive models.

## 6.2. Wind speed modeling using Autoregressive models

Wind data correspond to time series. Because the wind can be considered as a stochastic process, it is possible to propose models for time series modeling their behavior. Kennedy & Rogers (2003) suggest that the wind stochastic process is not purely random and successive values of the speed is not distributed independently. There are trends and seasonal components that confer some deterministic behavior of the wind (Kennedy & Rogers, 2003).

In this way, Kennedy and Roger (2009) represent a model for wind speed in the form of a time series which is composed by the sum of one seasonal component ( $S(t)$ ) and a random one ( $R(t)$ ). However it has been observed that the variable behavior of the variance in the wind is an important characteristic of wind data (the variance of the wind speed is higher in winter than summer), being necessary to normalize the probability component of the model. Kennedy & Roger then propose a time series model for the wind that can be observed in equation (6.3).  $V(t, m)$  corresponds to wind speed in time for the period  $m$ ,  $S(t, m)$  the corresponding seasonal component,  $R(t, m)$  a normal random variable (Kennedy & Rogers, 2003). Karki and Po used a similar approach in their model to estimate the reliability of the electrical system in the presence of wind turbines (Karki & Po, 2005).

$$V(t, m) = S(t, m) + R(t, m) \quad (6.3)$$

Because the standard deviation of the average wind speed is not equal for all months of the year, the stochastic process  $R(t)$  is not stationary. This hinders their modeling so it is necessary normalize using the standard deviation for the period considered in the

seasonal component  $S(t)$ . Then the variable  $\tilde{R}(t)$  normalized and stationary can be modeled by an autoregressive model like AR, ARMA, among others.

### 6.2.1. Autoregressive models

The concept of time series can be used to generate synthetic wind and predict the behavior of wind speed in the short term. Wind speed tends to correlate with previous values of that speed. For this reason, ARIMA (Auto-Regressive Integrated Moving Average) and simplifications (eg: Model ARMA or AR models) are used to model and predict the wind speed. Peiyuan used to model various ARIMA models based on sets of wind data from an offshore wind farm in Denmark Peiyuan, Pedersen, Bak-Jensen, & Zhe, 2010). ARIMA models of a process  $Y(t)$  nonstationary can be defined as the equation (6.4).

$$\left(1 - \sum_{i=1}^p \varphi_i B^i\right) (1 - B)^d Y(t) = \theta_0 + \left(1 - \sum_{i=1}^q \theta_i B^i\right) a(t) \quad (6.4)$$

Where  $\varphi_i$  are AR coefficients,  $\theta_i$  mobile average coefficient (MA),  $a(t)$  a white Gaussian process (white noise) with average 0 and variance  $\sigma_a^2$ . The parameter  $\theta_0$  represents a deterministic tendency when  $d > 0$ . When  $d = 0$  ARIMA process is reduced to a un ARMA model, in addition when  $q = 0$  the model is reduced to AR model and when  $p = 0$ , the model is reduced to a MA model (Peiyuan, Pedersen, Bak-Jensen, & Zhe, 2010).

## 7. ADDING WIND POWER PLANTS AND REDUCING VARIABILITY

The variability and the difficulty of predicting the wind speed can cause significant variability in the generation of a wind farm. This can present major challenges for operators of electric systems on the dynamic behavior of the system.

Although there are marked trends, the wind tends to have significant variations which generate gusts of wind power, interspersed with periods of little or no generation. This is confirmed by observing the frequency distributions for the generation of a wind farm, which shows that the zero generation components and maximum generation are very important compared to other components. Figure 7-1 shows a graph for the probability distribution for the generation of a wind farm for a year. It is observed that the generation component nil and the maximum generation component (100% nominal capacity) has an occurrence of a 22.09% and a 25.04% respectively, much greater to the rest of the power components exceeding zero and minors hundred per cent.

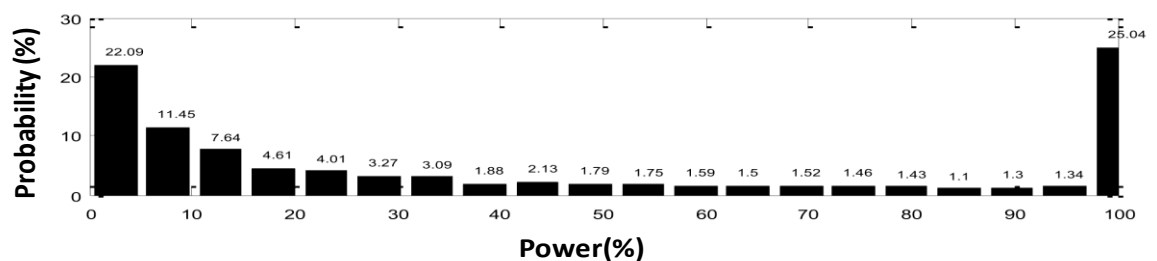


Figure 7-1 – Probability distribution for hourly power generation for a wind farm for an entire year

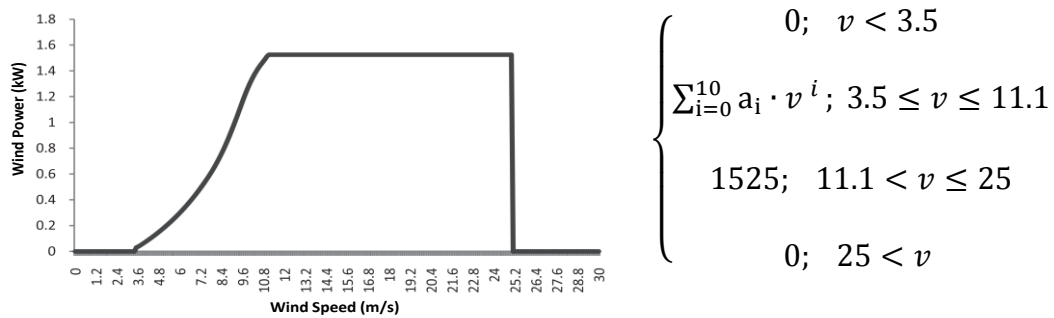


Figure 7-2 – Power curve for a wind generator (REPower MD77 generator with a 1,525 kW rating)

This behavior is due to the shape of the power curve of wind generators, which has a lower cutting speed and a superior cutting speed. Under the lower cutting speed the generator does not generate electricity, while on the higher cutting speed, the generator generates an output equal to the nominal power, no matter how the wind speed increases. Moreover, given an upper speed limit (high to superior cutting speed), the generator stops operating due to security issues. Figure 7-2 shows a power curve by way of example, for a generator REPower MD77 of 1.525 kW nominal, where lower cutoff speed corresponds to 3.5 m/s and higher cutting speed to 11.1 m / s. Above the 25 m / s the generator power generation takes zero value for safety reasons.

### 7.1. Spatial correlation and variability of wind generation

The decreasing correlation that the wind speed shows when the geographical distance between two wind farms increases can compensate in some way the "bad behavior" of wind generation compared to conventional technologies. If the wind speed from two

different and faraway places are compared, the correlation between two time series is very low (Apt, 2007; Burton, et al., 2001).

If different wind farms are installed considering the geographical dispersion of the generation, the probability of no generating electricity considering the aggregate generation is very close to zero (Kirby & Milligan, 2008). The wind generation is not completely intermittent considering the geographical dispersion and the effect of "smoothing" that the dispersion causes the generation of wind farms added (Noorgard, 2004).

Several studies have shown that adding wind generation plants in different parts of the system, the variability of aggregate generation is reduced to more plants and more distance between them (Archer & Jacobson, 2007; Czisch & Ernst, 2001; Giebel, 2000; Kennedy & Rogers, 2003; Milligan & Porter, 2005).

The variability of aggregate wind plants is less than the variability of each individual plant. The zero generation components and maximum generation in the frequency distribution graph is reduced as wind power plants with reduced correlation in their generation are added to the total generation. This effect can be observed in a Fourier analysis, where you will see that the turbulent components of the spectrum will be reduced as wind farms are added to the mix of generation (Katzenstein, et al., 2010).

While this is not enough to say that wind power plants can provide firm capacity added to the system, it is evidence that adding more plants uncorrelated the system is less subject to frequency regulation requirements, reducing compensation costs and the use of reserve capacity of the system, improving its reliability (Katzenstein, et al., 2010).

## **8. GENERATION OF SYNTHETIC DATA AND CALCULATION OF AGGREGATE POWER OF WIND FARMS**

The availability of detailed wind data in Chile is scarce. Currently there is no policy characterization of the resource at the national level, which establishes an important barrier to the development of wind projects in the country. Despite this, wind power, with the small hydro and biomass, has become one of the more developed unconventional renewable generation technologies in the country.

Moreover, wind power is perceived widely as a generation technology complex to integrate to power systems on a large scale due to the variability of his generation. For this reason, it is of interest to study the effect of aggregation of distant wind farms generation. To this end, the synthetic generation of data for wind speed is of great relevance.

This study modeled a national park wind generator, considering various wind projects operating or to be installed in the near future in the country. Wind time series were modeled to calculate synthetic plant factors for such projects, using mesoscale data according to location and detailed wind measurement stations. This information was later used to study the effect of aggregating the generation on the variability.

### **8.1. Data**

The data used for modeling corresponded to a set of detailed average wind speed data, with a 10 minutes resolution for a full year to various parts of north - central region. It also used mesoscale data based on satellite information to the locations of all

generation projects. Finally, we considered data generation technology as the height of generators, power curve, distance between towers generation, etc.

### **8.1.1. Series de tiempo para la velocidad del viento**

In the research conducted by Watts and Jara (2011) it was used series of wind speed averages for intervals of 10 minutes for eight locations on the northern and south-central Chile. These data correspond to data generated from a campaign to characterize the wind patterns in the northern and central Chile, organized by the National Energy Commission (CNE), the German Technical Cooperation Agency (GTZ)) and the program the United Nations development Programme (UNDP). These data were used as the backbone for the generation of synthetic wind data.

The information is use to model the seasonal components, generating synthetic wind data with these components. We considered that these data are representative of the wind profiles facing the wind projects in Chile, as these are often located near the coast, as in the case of measuring stations considered. A summary of the location information of measuring stations considered can be seen in Table 8.1.

Table 8.1– Principal information about wind speed measurement locations in the northern and central Chile

Station	Latitude	Longitude	$\Delta t_s$ [min]
Carrizalillo	29° 2'29.00"S	71°23'45.00"O	10
Cebada Costa	31° 01'53.94" S	71° 37'4284"O	10
Cerro Juan Pérez	30°56'50.46"S	71°33'48.84"O	10
Faro Carranza	35°32'32.30"S	72°35'20.90"O	10
Lengua de Vaca	30°14'51.18"S	71°37'43.38"O	10
Llano de Chocolate	28°57'50.70"S	71°14'34.08"O	10
Loma del Hueso	28°54'28.38"S	71°27'1.44"O	10
Punta los Choros	29°14'17.58"S	71°25'48.72"O	10



The data sets correspond to the average velocity values in 10 minutes resolution for a full year of measurement. Measuring stations considered were: Carrizalillo, Cebada Costa, Cerro Juan Pérez, Faro Carranza, Lengua de Vaca, Llano de Chocolate, Loma del Hueso y Punta los Choros. The location of the stations in the Chilean territory on the map can be seen in Table 8.1. The main relevant statistics as the mean (between 3.74 m / s and 6.09 m / s at 40 meters), standard deviation (between 2.22 m / s and 3.98 m / s at 40 meters) and measuring height (between 11 m and 40 m) are presented in Table 8.2.

Table 8.2 - Annual Statistics for measurement stations (Watts &amp; Jara, 2011)

<b>Height</b>	<b>Average [m/s]</b>	<b>Stad. Var. [m/s]</b>
<b>Carrizalillo</b>		
<b>40 [m]</b>	4.66	2.48
<b>20 [m]</b>	4.4	2.35
<b>11 [m]</b>	4.18	2.25
<b>Cebada Costa</b>		
<b>20 [m]</b>	5.65	3.56
<b>11 [m]</b>	5.26	3.4
<b>Cerro JP</b>		
<b>20 [m]</b>	4.44	2.92
<b>11 [m]</b>	4.23	2.66
<b>Faro Carranza</b>		
<b>40 [m]</b>	5.79	3.42
<b>30 [m]</b>	5.47	3.24
<b>20 [m]</b>	5.15	3.06
<b>Lengua de Vaca</b>		
<b>20 [m]</b>	6.09	3.98
<b>11 [m]</b>	5.71	3.73
<b>Llano de Chocolate</b>		
<b>20 [m]*</b>	6.09	3.98
<b>Loma del Hueso</b>		
<b>20 [m]</b>	6.08	2.86
<b>11 [m]</b>	5.32	2.6
<b>Los Choros</b>		
<b>20 [m]</b>	3.98	2.22
<b>11 [m]</b>	3.74	2.24

### **8.1.2. Agenda of wind projects in Chile**

To determine the projects to be modeled the information contained in the System of Environmental Impact Assessment of Chile (SEIA) was reviewed. In February 2010, SEIA information indicated that there were 169 MW of installed wind capacity available while there were 1,330 MW of wind capacity of approved projects to be constructed and 683 MW of wind projects in the evaluation process, totaling a generating potential of 2,182 MW wind farm to be installed in the future. These projects are or will be connected to the main interconnected systems of the country, the central grid (SIC) and the Northern Interconnected System (SING). Figure 8-1 shows the main features of wind projects by the interconnected system (SIC and SING).

Table 8.2 presents the main information about the projects considered in the model. The information consists of the main characteristics of projects, including its total installed capacity, installed capacity per turbine, the turbine model, the spacing between each turbine and tower heights. This information is used to model wind farms.

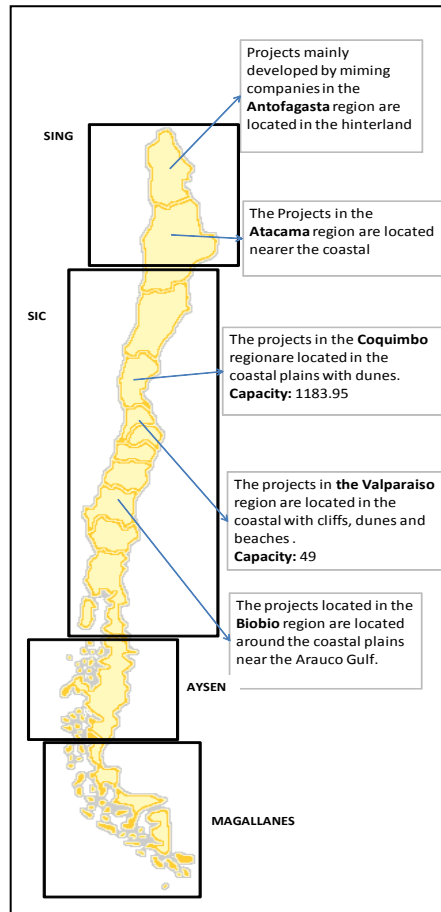


Figure 8-1 – Map of Chile including general description about wind projects modeled

Table 8.3 - Principal information about wind energy projects modeled

Project	Project Nº	Region	Uni. Cap. [MW]	Turbine Nº	Cap. [MW]	Height [m]	Turbine Sep. [m]	Turbine Type	System
Quillagua	1	2	2	50	100	80	600	Vestas V80 **	SING
Minera Gaby	2	2	2	20	40	80	650	Vestas V80 **	SING
Calama	3	2	2*	125	250	80	500	Vestas V80 **	SING
Valle de los vientos	4	2	3	33	99	119	600	Vestas V112 **	SING
Altos de Hualpén	5	3	2	10	20	67	600	Vestas V80	SING
Señora Rosario	6	3	1.5	56	84	80	600	GE 1.5xle	SING
Totoral	7	4	1.65	27	46	70	600	Vesta V82	SIC
Canela	8	4	1.65	11	18.2	70	220	Vestas V80	SIC
Monte Redondo	9	4	2	24	48	80	600	Vestas V80 **	SIC
Canela II	10	4	1.5	40	60	80	600	GE 1.5xle	SIC
Punta Colorada	11	4	2	18	36	80	600	Vestas V80 **	SIC
Talinay	12	4	2*	243*	486**	80	600	Vestas V80	SIC
Hacienda Quijote	13	4	2	13	26	80	600	Vestas V80 **	SIC
Las palmeras	14	4	1.5	69	103.5	80	600	GE 1.5xle	SIC
El pacífico	15	4	2	36	72	105	600	Vestas V80 **	SIC
La gorgonia	16	4	2	38	76	105	600	Vestas V80 **	SIC
La Cachina	17	4	2	33	66	105	450	Vestas V80 **	SIC
El Arrayan	18	4	2.3*	44	101.2	113	600	ENERCON E70 **	SIC
Laguna Verde	19	5	2	12	24	80	600	Vestas V80 **	SIC
Punta Curaumilla	20	5	1.8	5	9	80	600	Vestas V100 **	SIC
Las Dichas	21	5	2	8	16	105	450	Vestas V80 **	SIC
Lebu	22	8	0.75	9	6.54	50	450	UGE 750 H **	SIC
Chome	23	8	2	6	12	80	600	Vestas V80 **	SIC
Arauco	24	8	2	50	100	80	600	Vestas V80 **	SIC
Lebu Sur	25	8	2	54	108	80	600	Vestas V80 **	SIC
Cabo Negro	26	12	0.75	3	2.25	50	450	UGE 750 H **	Magallanes

\* Explicit information SEIA  
 \*\* Inferred based on information SEIA

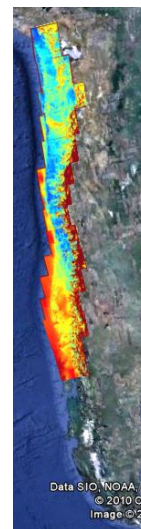


### 8.1.3. Mesoscale data and georeferencing

The lack of detailed information is a major problem in assessing wind generation projects and estimate the impacts on the electricity networks of these projects. Because of this lack of information, different alternatives are being carried out in order to compensate for this problem. One is the study of mesoscale led by the department of geophysics at the University of Chile, at the request of the CNE. This study models the wind resource using numerical methods and satellite data, establishing color maps, which plotted the average wind speed (CNE, 2009c). Detailed information about the study can be obtained on its website (CNE, 2010).

Table 8.4 - Reference information for the projects modeled including mesoscale map

Proyecto	Data ref.	Mean [m/s]	Heigth [m]	Rug. Coef
Quillagua	Carrizalillo	4.79	75	0.065
Minera Gaby	Carrizalillo	4.64	75	0.100
Calama	Loma del Hueso	6.63	75	0.073
Valle de los vientos	Loma del Hueso	6.29	75	0.113
Altos de Hualpén	Carrizalillo	7.35	75	0.080
Señora Rosario	Carrizalillo	3.8	75	0.127
Totoral	Cebada Costa	5.5	75	0.152
Canela	Cebada Costa	5.48	75	0.164
Monte Redondo	Cebada Costa	6.6	75	0.161
Canela II	Cebada Costa	5.52	75	0.164
Punta Colorada	Carrizalillo	3.59	75	0.156
Talinay	Cebada Costa	5.83	75	0.106
Hacienda Quijote	Cebada Costa	6.04	75	0.163
Las palmeras	Cebada Costa	6.09	75	0.098
El pacífico	Cebada Costa	7.04	75	0.157
La gorgonia	Cebada Costa	6	75	0.093
La Cachina	Cerro Juan Perez	5.24	75	0.058
El Arrayan	Lengua de Vaca	5.38	75	0.152
Laguna Verde	Loma del Hueso	8.87	75	0.190
Punta Curaumilla	Faro Carranza	8.99	75	0.172
Las Dichas	Faro Carranza	4.87	75	0.202
Lebu	Faro Carranza	7.35	75	0.208
Chome	Faro Carranza	7.57	75	0.108
Arauco	Faro Carranza	7.71	75	0.124
Lebu Sur	Faro Carranza	7.34	75	0.197



The information in this study is combined with the georeferencing tool "Google Earth" to locate the projects considered by the mesoscale information and the measuring stations location listed in Table 8.1. In this way, it was assigned the series of real wind nearest each one of the projects evaluated, which was used to model the seasonality of wind. This information combined with mesoscale (mean and standard deviation) was used to generate synthetic wind and estimate detailed energy generation. The allocation of detailed data (measurements) and mesoscale data for each project was according to its position shown in Table 8.4.

## 8.2. Assumptions considered

Disaggregated data of average wind speed measured in situ were extrapolated to the heights of the towers of wind turbines, ie, 67 m., 70 m., 80 m., 105 m., 113 m. and 119 m. For this we use the shear profile and the parameter values for the projection

calculated by Watts and Jara for these data (Watts & Jara, 2011). The data were presented at heights of 11m, 20 m. and 40m. We used the information to 40 m. for being the closest to the heights required for the simulation.

For mesoscale data, these were available for 10 meters. and 75 m. With this information we estimated the shear parameter for each location to study and then extrapolate the average speeds to the right height using the 75 m. data to the heights required by the towers of the wind generators mentioned above.

Furthermore, mesoscale information provided charts probability distributions of the wind resource at 75 m. tall. These charts were tabulated by observation and approximate graphs were obtained for the empirical probability distributions. We applied a method of maximum likelihood approach assuming a typical statistical behavior Weibull curve for probability distributions. The Weibull parameters associated with the empirical distributions were estimated. The shape parameter ( $\alpha$ ) and the scale parameter ( $\beta$ ) of the Weibull distribution were used to calculate the standard deviation of the data according to equation (8.1). It is assumed that the standard deviation, unlike the average velocity, does not vary importantly with height, by what is considered constant (Burton, et al., 2001).

$$\sigma = \beta \sqrt{\Gamma\left(\frac{2}{\alpha} + 1\right) - \left(\Gamma\left(\frac{1}{\alpha} + 1\right)\right)^2} \quad (8.1)$$

Standard deviation and average wind speed data provided by the mesoscale model correspond to annual values. To generate data to collect monthly seasonal behavior the annual wind speed profiles for mean and standard deviation of the actual data

considered in the study were analyzed. A percentage profile with the percentage monthly deviation from the annual value as constructed. This profile describes the percentage deviation of the average annual rate or annual standard deviation for each month. With this deviation percentage values were estimated for each month for the mean and standard deviation.

### **8.3. Procedure and modelling**

The following step were followed to study the effect of aggregation of wind farms in Chile and to estimate the plant factor added to the potential generating facilities in the country: Analysis of wind data series, generation of synthetic data and calculation of wind generation for each park. With this procedure the behavior of wind generation and how this reduces variability by adding as many parks in the total wind generation were studied. The reduction in zero generation event indicate the existence of a base generation. In addition, we estimated the systemic capacity factor for all generators parks.

#### **8.3.1. Wind data series and mesoscale information analysis**

The real wind data series were analyzed and the frequency components of greater importance were estimated as shown in Figure 5-2, seeing that typically, the components of relevance correspond to the components of 24 hours, 12 hours and 5 to 8 hours, depending on the case. These components were isolated and translated into the time domain to be included as seasonal component  $S(t)$  as shown in equation (6.3). Because the seasonal component major component corresponds to the day - night we

calculate the standard deviation for the daily averages of each month in the data series. This deviation is used later to generate the component  $R(t)$  based on a series  $R(t)$  normalized.

The annual averages and standard deviations provided for wind mesoscale information were used to define the average and standard deviation of the final synthetic series generated for locations defined for each of the wind projects considered in the modeling.

### **8.3.2. Synthetic data generation.**

The process of generating synthetic data produce average wind speed in 10 minutes resolution for a full year for each of the locations of the projects considered in the model. The generation of synthetic wind made so that the generated data present a mean and standard deviation similar to those expected according to mesoscale information. Furthermore, the absence of better information, the synthetic wind series were scaled to the height of wind towers for each project, using the wind shear profile roughness coefficients estimated by Watts and Jara (2011) for the real wind data series (Watts & Jara, 2011).

Synthetic data generation was performed using an autoregressive model (AR) which derives from equation (6.4). An AR model is considered based on the evidence shown by Aksoy et al. (2004), Poggi et al. (2003) and Kennedy & Rogers (2003), where AR models adequately capture the variability shown for wind resource by reproducing the mean and standard deviation expected, using fewer parameters and computation time (Aksoy, Fuat Toprak, AYTEK, & Erdem Ünal, 2004; Kennedy & Rogers, 2003; Poggi,

Muselli, Notton, Cristofari, & Louche, 2003). This model fits well because the time interval between real measurements considered is 10 minutes. With longer intervals (eg 30 min or 1 hour) the result obtained with an AR model would not be of good expected quality. According to Poggi et al. (2003), AR models are able to adequately capture the positive correlation between data in a time series of the average wind speed, while being flexible enough to fit the main characteristics of the wind and accurate energy analysis .(Poggi, et al., 2003).

The model considered can be seen in equation (8.2) which consists of a model AR (1). We consider a model of order 1 because higher orders do not add significant precision results (Kennedy & Rogers, 2003).. The variable  $R(t, m)$  represents a normalized random variable generated when removing seasonal components of a series of real wind. With this variable  $R(t, m)$  using a linear regression in Matlab, the autocorrelation coefficient  $\alpha$  was obtained. With the known coefficient is possible to obtain the values of the error random variable  $e(t, m)$ , which distributed with mean zero and standard deviation estimate as each set of measured data used.

$$\tilde{R}(t, m) = \alpha \cdot \tilde{R}(t - 1, m) + e(t, m) \quad (8.2)$$

Then, when  $\alpha$  coefficient values and standard deviation of the  $e(t, m)$ , variable ( $\sigma_{\text{error}}$ ) were estimated, knowing well the seasonal components of each time series and the means and standard deviations of wind on the location of each project, it is possible to generate synthetic wind series which preserve the frequency properties of real wind data and are consistent with the mean and standard deviation of wind speed present in each project considered in modeling.

### Synthetic wind generation methodology

The methodology used to generate synthetic wind data from real average wind speed, knowing the correlation coefficient  $\alpha$  for each time series, the standard deviation of the component  $e(t, m)$  for the components seasonal time series in real used with the data from mesoscale wind speed average and standard deviation for each of the projects considered. The calculation methodology to use is the following:

1. Generate a random data set of normal distribution with mean zero and standard deviation equal to  $\sigma_{\text{error}}$  calculated from original  $e(t, m)$  data series.
2. Starting with a value  $R(t-1) = 0$  calculate the number  $R(t)$  using the series  $e(t, m)$  calculated in the previous step and coefficient  $\alpha$  according to equation (8.2).
3. Add the seasonal components  $S(t, m)$  obtained by Fourier analysis to the series  $R(t)$  generated, to obtain the variable  $V(t, m)$  as shown in equation (6.3)
4. Get the average and standard deviation of the data series generated and standardize the series so that the left with zero mean and standard deviation equal to 1
5. Multiply the number obtained in the previous step by the standard deviation of mesoscale data for the location of the project. Then add the average data obtained from the mesoscale.

This procedure should be considered for each project, using data based on average wind speed that are closest to the location of the project as indicated in Table 8.4. Data generation should be done monthly, and then assemble the different series of synthetic wind and get a series for a full year.

### 8.3.3. Calculation of electricity generation for wind parks

The model considers different wind farms, modeling wind turbine with their power and height curves, obtaining the total generation of the park as the aggregation of the generation of each individual turbine. The aggregate generation of all wind farms is obtained from the sum of the individual power generation park. Wind generation is calculated by evaluating the series of synthetic wind generated in the power curves of each wind turbine, considering the escalated wind data series at the height of each generator by the wind shear profile according to equation (8.3). For this, we used data from mesoscale to 10 m and 75 m and estimated the wind shear parameter for each particular location

$$\frac{v(z_2)}{v(z_1)} = \left(\frac{z_2}{z_1}\right)^k \quad (8.3)$$

The wind farms considered in the modeling were classified into four groups according to analyze their localization in regions of Chile. Projects in the 1st and 2nd region were grouped in the first set of analyzes, the projects of the 4th region in the second set of analyzes, the projects of the 5th region in the third set of analysis and the 8th region in a fourth group. Importantly, the project number 26 (cabo negro) was not considered due to its distance from the major Chilean electric systems (SIC - SING). Wind farms and turbines were arranged in matrix arrangement using Matlab, in order to consider effects of the distance between turbines and effects of loss by "shadowing" of turbines over others.

### 8.3.3.1. Space between wind turbines and losses

The distances between each of the turbines and wind movement through these distances were considered using the average wind speed. The model implemented in Matlab calculates the elapsed time between a row of generators of a wind with the wind and the same burst reaches the second row using the average wind speed. On this basis, the time series were displaced as applied to subsequent rows in the model, so as to reflect changes in generation between generators in a wind farm. The equations (8.4), (8.5) and (8.6) show the calculation of time between rows and displacement of the series of wind, with  $\bar{w}$  average wind speed,  $d_T$  the distance between generators and  $f_m$  the time interval between series data of wind (10 minutes).

$$t = \frac{\bar{w}}{d_T} \quad (8.4)$$

$$n = \frac{\text{integer part}(t)}{f_m} \quad (8.5)$$

$$w(j) = w(j - n), \forall j > n \quad (8.6)$$

It was also considered a 10% loss in the generation of each wind farm due to mechanical losses, shadow effect generators and network losses.

## 8.4. Results and discussion

The algorithm previously described was implemented to generate 25 sets of synthetic wind data for one year with a resolution of one reading every 10 minutes, which were used to provide detailed information to model the behavior of the wind. Different sets

of real wind were used to generate synthetic wind series, depending on the location of modeled projects.

Figure 8-2 shows the results of the synthetic generation of data compared to the series of real wind for one month data. Upper wind trajectory shows the graph of the series of real wind, while the lower wind trajectory shows the synthetic wind graph.

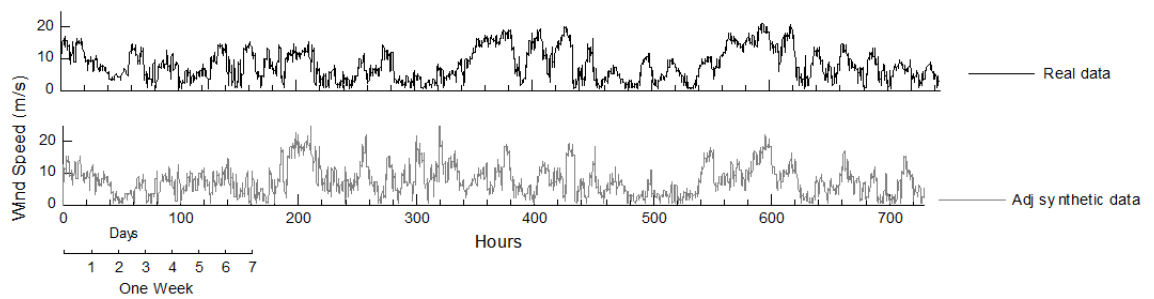


Figure 8-2 - Wind Trajectories for real data (up) and synthetic data (down) in

m/s

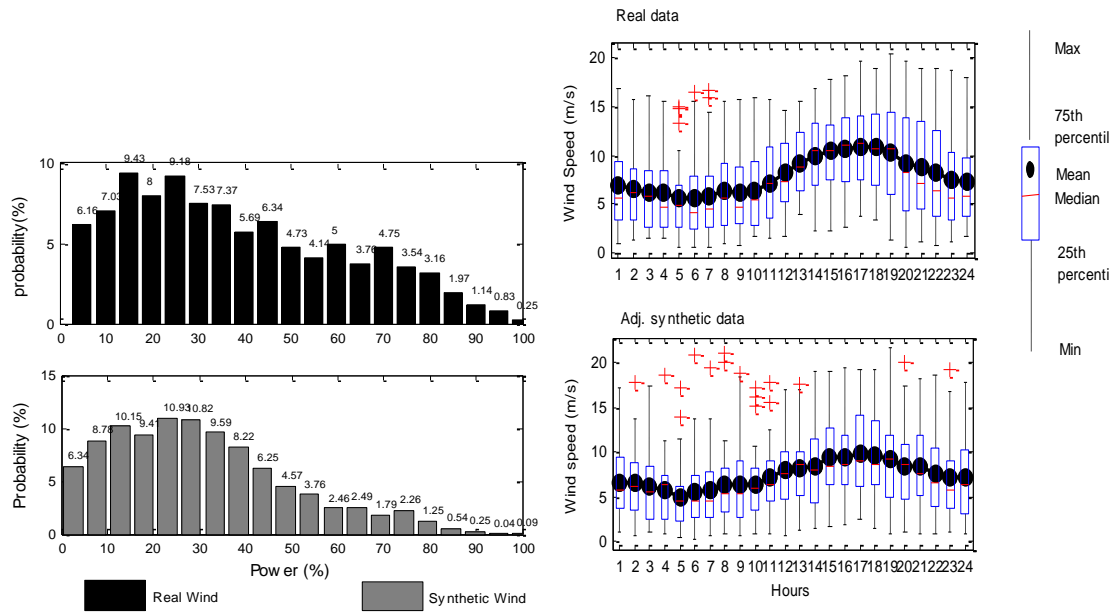


Figure 8-3 - Probability distribution (left) and daily profile (left) for real and synthetic data

On the other hand, Figure 7 shows the empirical probability distribution for the real wind and the synthetic wind series and the daily profiles (hourly averages for a day average) for both series. It is observed that the daily profile of the synthetic data preserved the daily shape as expected, showing the trend among day and night where the wind speed tends to drop during the night and up during the day. The probability distribution of the series of synthetic wind fits the expected form, seeing that follows a shape similar to the Weibull distribution. Table 8.5 presents the mean and standard deviation for both series seeing that the values obtained are very similar. The average speed for the actual series is 7.35 m/s while the average for the synthetic series is 7.44 m/s. The standard deviation for the number of true wind is 4.86 m/s while for the series of synthetic wind is 4.71 m/s

Table 8.5 - Statistical parameter for a real and corresponding synthetic wind data

Data	Mean (m/s)	Std (m/s)
Real	7.35	4.86
Sintética	7.44	4.71

Figure 8-4 shows the number of periodogramas for real and synthetic wind. It is observed that the main seasonal components 24 hours and 12 hours are maintained for both series of wind, so that the series of synthetic wind maintains its behavior in frequency compared to the actual series that originated it.

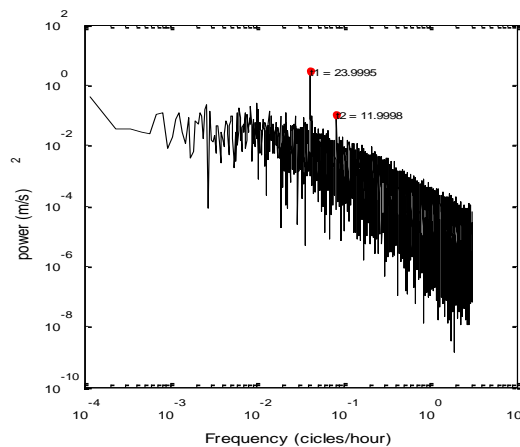
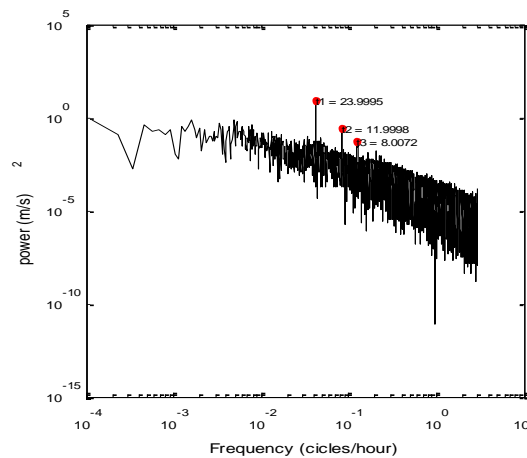


Figure 8-4 - Periodogram for real wind data (left) and synthetic wind data  
(right)

#### **8.4.1. Wind power aggregation**

The data generated by the algorithm for synthetic generation of wind were used to calculate the generation of various wind projects, considering the height of the tower, the appropriate power curve for each generator and the distance between generators. Figure 8-5 shows the synthetically generated wind trajectories for three wind farms. It is appreciated as the three trajectories show different behaviors, however, being checked, all of them presented the appropriate seasonal components (24 hours and 12 hours) as well as a statistical behavior expected (Weibull distribution).

Figure 8-6 shows the power generation for a wind farm and the corresponding wind series used for the project. It can be seen the effect of the wind turbine over the power output, showing how the generation passes from non-zero values to periods without generation or maximum generation. The peaks of wind speed correspond to the maximum generation, while lower speeds near zero are translated into a null generation.

Figure 8-7 shows the periodogram for the power generated by a wind farm (left) and for the total national aggregate. It is noted that the seasonal components are maintained between the generation of a wind farm and wind farms of total aggregates.

The addition of wind generation to the mix causes the maximum generation and no generation hours will decrease as new parks are being added. This shows how the addition of park compensates the variability of total wind generation. Table 8.6 shows

the maximum generation hours and zero for a park, a group of parks and parks total modeled. It is observed that the occurrence of null generation is reduced from 164 hours to 24 hours if a considerable number of parks are group (12 parks) and then to 0 hours to total parks considers generators. This reveals that the national aggregate wind generation never reaches a zero value, can be said that there is a small base generation capacity by considering all wind farms.

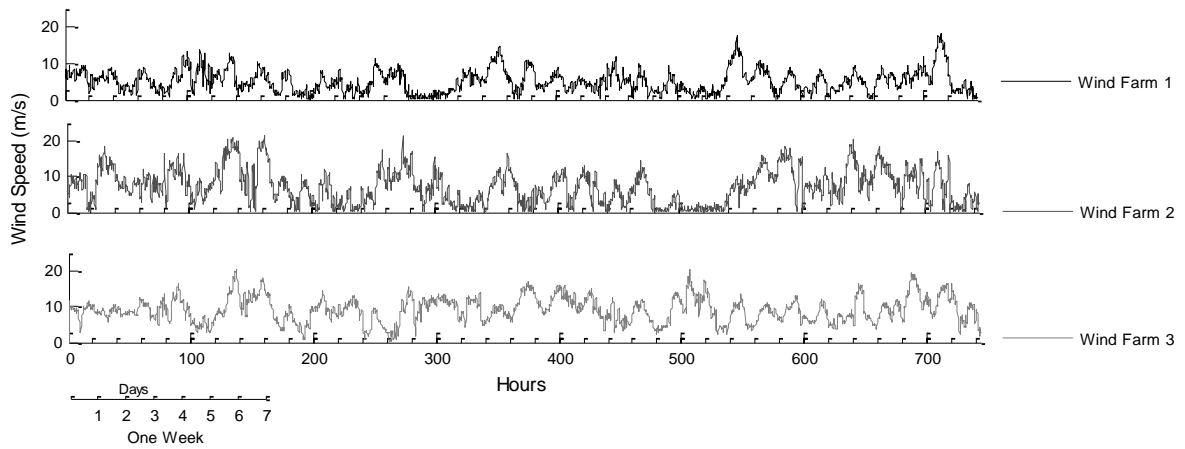


Figure 8-5 - Wind speed trajectories for three different wind farms

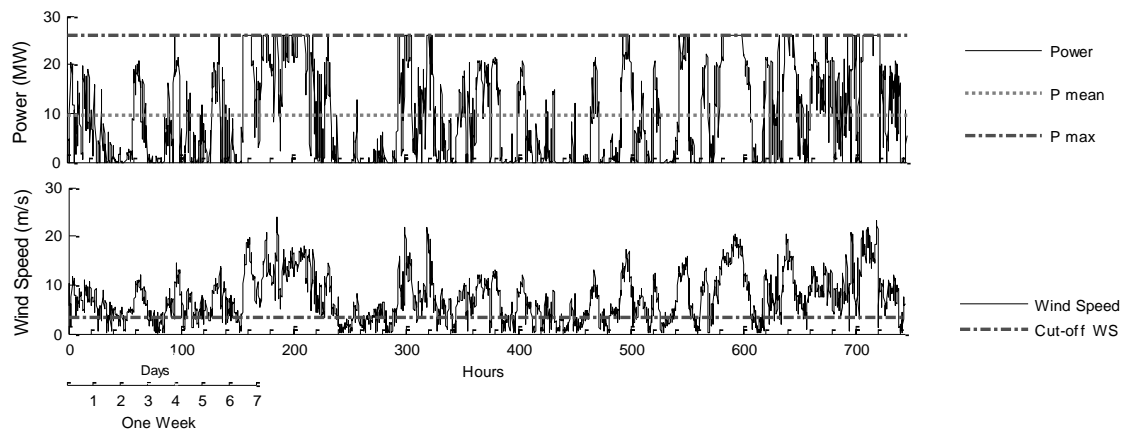


Figure 8-6 – Wind speed trajectory and corresponding electric power generated for a wind farm

Table 8.6 - Max and null generation number of hour for a wind park, a group of parks and the total in the country

Potencia	Time	
	100% Capacidad	Generacion nula
<b>Parque</b>	120 h	164 h
<b>Grupo</b>	10 min	24 h
<b>Total</b>	10 min	0 h

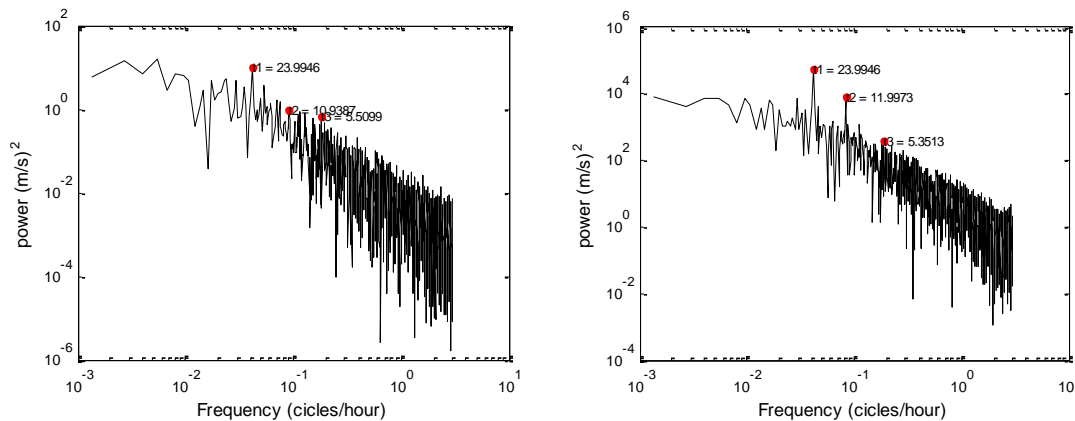


Figure 8-7 - Periodogram for electric power generation for a wind farm (left) and the total national (right)

The reduction of episodes of no generation and maximum generation can be seen clearly by observing the trajectories of wind generation for a wind farm, a group of parks and parks total. In Figure 8-8 can be seen that the curve for a wind farm generation often touches the null value and maintains maximum generation appreciable time intervals. However, in the case of the national total aggregate (25 parks), the graph

never touches the null value and can be seen a generation of base which is maintained through the entire interval of tempo (one month of data).

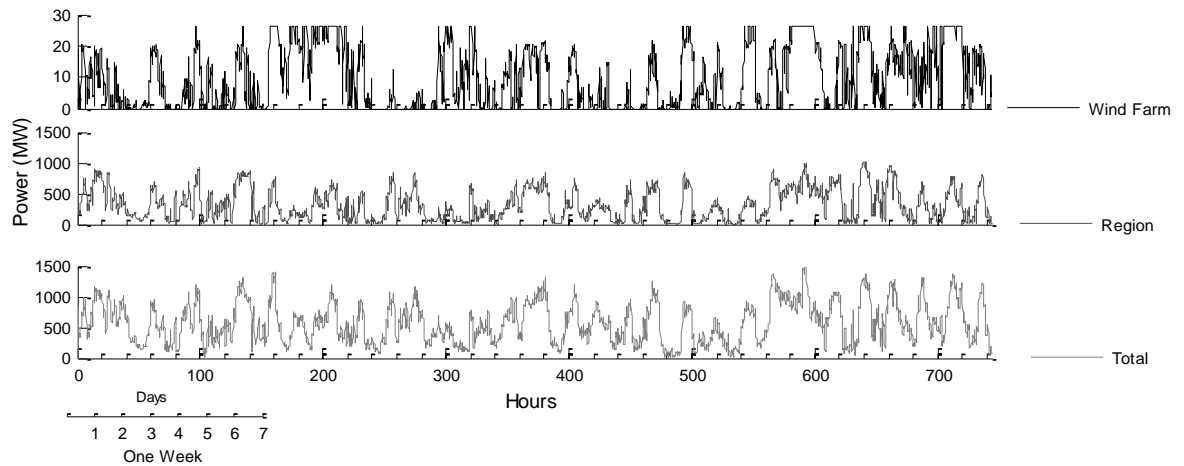


Figure 8-8 - Power generation for a wind farm (up), a group of wind farms (middle) and the total for the country (down)

The behavior of wind generation described above can be corroborated from the probabilistic approach. Figure 8-9 shows how the probability distribution of wind generation of a wind generation exhibits important components of zero and maximum generation. However, as observed in Figure 8-8 (below), as new parks are added to the total electricity generated from wind, the null and maximum components begin to decrease so that the probability distribution for total parks will be closer to a normal distribution, with maximum generation and events with very low probability zero.

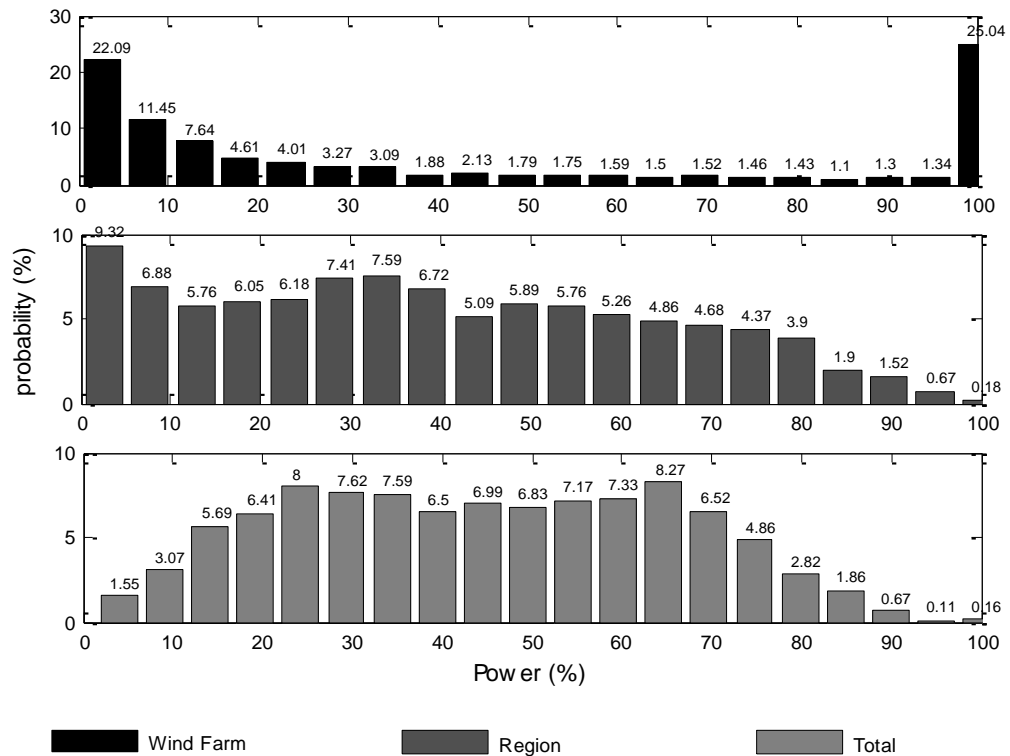


Figure 8-9 - Probability distribution for a wind farm (up), a group of wind farms (middle) and the total for the country (down)

Another important conclusion is the reduction of turbulent component in the wind power generation when more wind farms are aggregated to the system. The rapid variation of wind power generation will be less important when more wind farms are aggregated to the the system. The Figure 8-10 shows a periodogram graph with the power spectrum for the wind power generation normalized with the average power value for each serie. The black graph shows the frequency spectrum for the generation of a wind farm, the blue graph the frequency spectrum for a group of wind farms (12) and the red graph for all the projects modeled (25). It is possible to see that the section of the graph corresponding to the turbulent component, this is the Kolmogorov

spectrum (frequencies from 10<sup>-1</sup> to 10<sup>1</sup> cycles /hour). It is possible to see that the slope of the section of the graph increase its value from the wind farm to the total generation modeled. This means that the energy contents in this components is reduced when more wind farms are aggregated to the system

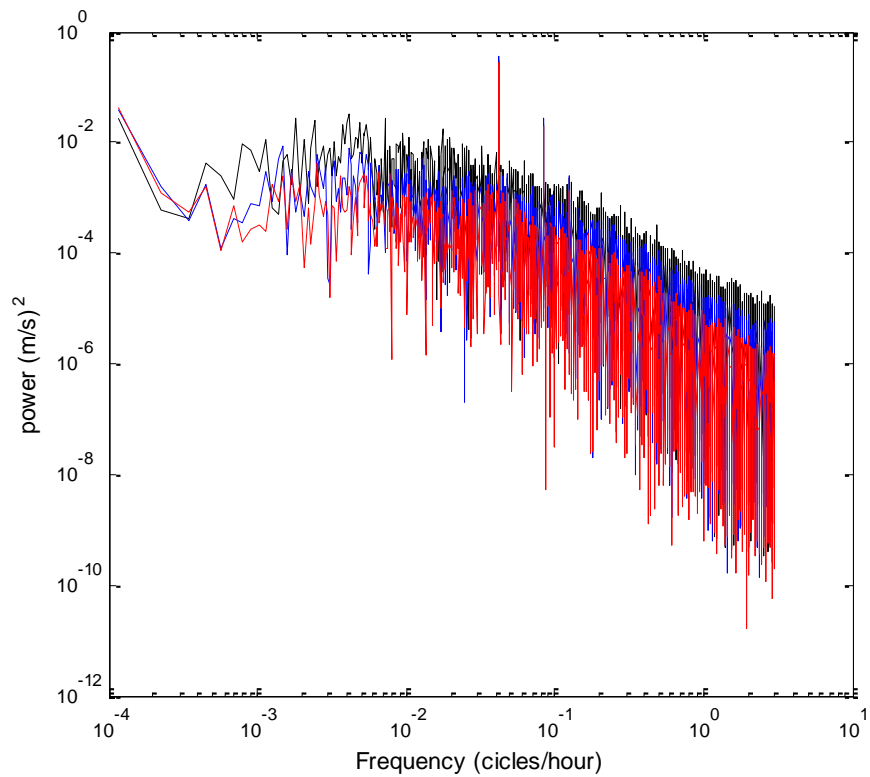


Figure 8-10 - Comparison of turbulent component for wind power generation of a wind farm (black), a group of 12 wind farms (blue) and all the projects modeled (red)

### 8.4.2. Capacity factor estimation

Table 8.7 shows the capacity factors calculated for a wind farm, to an entire region and ultimately for the whole park modeled. The systemic capacity factor is equal to 22.9% this value being greater than for the case of a smaller group of parks (12) with a plant factor of 21.5, considering all the modeled parks. If only is considered wind parks operative and future wind parks with a capacity factor over 20%, the systemic capacity factor improve to 29.25% and for a smaller group (12) with a capacity factor of 0.276. An operative wind far like Monte Redondo present a capacity factor of 26.1% in the simulation, while during 2010 the same park shows a real capacity factor of 24.8%<sup>7</sup>. This difference can be due a greater value of losses in the real operation of the wind farm y/o the difference in the wind resource modeled and the wind resource present in the area. However, the simulation shows capacity factor values expected and according with the real wind resource and the generation technology used in the wind power generation in Chile.

Table 8.7 - Capacity factor for a wind farm, a group of wind farms (12) and the total for the country

		<b>Wind park</b>	<b>Group</b>	<b>Total</b>
<b>Capacity factor</b>	<b>%</b>	26.1%	27.6%	29.2%

---

<sup>7</sup> Based in information provided for CDEC – SIC Chile.

Table 8.8 shows the detail of the generated energy, installed capacity, power and average plant factor for each of the projects modeled. There is great variation in plant factors. However as seen in Table 8.7, the tendency to add projects, is that the systemic plant factor tends to increase its value.

Table 8.8 - Detailed information for project modeled: Installed capacity, capacity factor and average power

Project N°	Energy [MWh]	Capacity [MW]	Capacity Factor [%]	Average Power [MW]
1	91,220.83	100	10.41%	10.41
2	31,002.29	40	8.85%	3.54
3	534,561.13	250	24.41%	61.02
4	270,887.75	99	31.24%	30.92
5	53,382.59	20	30.47%	6.09
6	95,191.76	84	12.94%	10.87
7	93,097.62	46	23.10%	10.63
8	35,585.47	18.2	22.32%	4.06
9	109,795.72	48	26.11%	12.53
10	158,170.78	60	30.09%	18.06
11	23,811.65	36	7.55%	2.72
12	709,143.07	486	16.66%	80.95
13	56,384.49	26	24.76%	6.44
14	329,617.26	103.5	36.36%	37.63
15	190,475.93	72	30.20%	21.74
16	149,474.03	76	22.45%	17.06
17	105,865.01	66	18.31%	12.09
18	167,412.70	101.2	18.88%	19.11
19	90,204.16	24	42.91%	10.30
20	37,681.81	9	47.80%	4.30
21	22,473.66	16	16.03%	2.57
22	25,670.73	6.54	34.70%	2.27
23	33,876.30	12	32.23%	3.87
24	301,025.97	100	34.36%	34.36
25	304,699.47	108	32.21%	34.78

## 9. CONCLUSIONS

According to the generation and capacity factor estimates obtained from a parallel survey (Watts, 2009) produced by our team, the mini hydro and geothermal energies entail more economic setting up opportunities as opposed to wind power equivalents. However, while being placed right behind conventional technologies, wind energy appears to be the most economic option enjoying no major barriers and restrictions when it comes to considering its location and exploitation prospects. Its potential is distributed throughout a number of diverse areas, subject to no water flow restrictions of any kind and suffering from no high costs when it comes to identifying the exact location of the resource vis-à-vis the plus factors enjoyed by mini hydro and geothermal technologies.

Chile's seabed configuration and the significant depth readings along its coastline rule out – for most of the areas considered in the survey - any offshore wind power generation technology facilities. However, and on the same geographical basis, the onshore wind power generation technology presents a significant development potential.

The wind flows analyzed here denote maximum average performance ratings associated to warm temperature, with a daylight daily profile whereby the highest speed readings are at around 4 PM. The potential is located next to the coastline, in areas with high cliffs that appear suitable for the setting up of power generation technologies at relatively low costs.

Of all eight stations, six offer very promising potential and only one has produced very low results. The readings undertaken suggest a larger wind power potential at the stations known as “Loma del Hueso” with a 44.8% theoretical capacity factor and an average wind speed of 7.76 [m/s] at 61.5 m high. Estimations at Lengua de Vaca, Cebada Costa, Faro Carranza and Llano de Chocolate<sup>8</sup> suggest a high enough potential with capacity factors above 30% and average wind speed above 6 [m/s]. However, there is a growing need for a quality wind power generation map coupled with public domain data suitable for a better evaluation of the resource on these and other areas throughout Chile.

Wind power generation is already a competitive option vis-à-vis other non-conventional renewable energies. The currently available wind power generation technologies are mature and reliable enough. Their pricing over a medium-term horizon is likely to become even more competitive with conventional media. This achievement appears particularly feasible thanks to the branching into the 1.5 MW and higher market segment by China and to the Non Conventional Renewable Energy (NCRE) Law which calls for the use of these technologies. The expansion of the wind power generation equipment park in year 2009 and the number of wind power generation projects that are either approved or currently going through the environmental impact approval motions is very much in line with the foregoing conclusions.

---

<sup>8</sup> Since there is only one measurement available for the latter zone it was not possible to arrange a data escalation, thus we believe its potential is even bigger and therefore this energy measurement underrates the generation potential.

The wind resource natural behavior and properties should be considered when assessing and modeling the resource. These properties correspond to the seasonal wind behavior and the positive correlation of wind speed in short periods of time. To demonstrate the relevance of these elements is implemented a model to generate large amounts of data and modeling synthetic wind parks existing or to be installed in Chile. To achieve an effective modeling, real data for average wind speed for a full year were used (10 minutes resolution). This information was used to obtain the seasonal components of the wind in the coastal area of north and central Chilean territory. Data from mesoscale was also used to provide aggregate statistical information about wind behavior in areas where wind generation projects are located. This information was used to generate synthetic wind series to address the lack of detailed information on the conditions of the wind resource at the point of location of wind projects.

The synthetic wind data generation was achieved using a first order autoregressive model AR (1) and analysis in the frequency spectrum. Wind farms are modeled as matrix arrangements, considering the distances between wind turbines and the heights of the towers themselves. Appropriated power curves for each generator was considered and the wind data were scaled to the height of the towers of generation using the coefficients of terrain roughness for the wind shear profile.

It was observed that the synthetic data generated retained the properties in the frequency spectrum of the real data from which were generated. Synthetic data shows expected statistical properties, showing a Weibull distribution, with a mean and standard deviation very similar to the data supplied for the mesoscale information.

The electrical output calculated by the model exhibits interesting features. The generation of a single wind farm tends to have frequent periods of no generation and maximum generation due to the behavior of wind turbine generation (lower and higher cutting speeds). When calculating the aggregate generation, generators were grouped by their geographical location and then the total aggregate generation for the country was calculated. The total generation shows that the occurrence of zero and maximum generation is drastically reduced, seeing that the total aggregate generation never reaches zero values and exist a small base capacity. It is observed that the probability distribution of wind generation tends to the normal distribution when a greater number of parks were added. Also, the turbulent components are reduced when more wind farms are aggregated to the system, increasing the slope of the Kolmogorov spectrum in the periodogram when a wind farm is compared with a group of wind farm (12) and with the total projects modeled (25).

Finally we obtain the value for the capacity factor added for national wind farm, obtaining a value of 29.2% whereas 10% of losses due to mechanical losses, shadow effect of wind turbines and electrical losses, considering only operative parks and future parks with a capacity factor over 20%. It is observed that as you add more parks, capacity factor improve its value, which is consistent with the statistical behavior of the generation.

## BIBLIOGRAFÍA

Aksoy, H., Fuat Toprak, Z., Aytek, A., & Erdem Ünal, N. (2004). Stochastic generation of hourly mean wind speed data. *Renewable Energy*, 29(14), 2111-2131.

Apt, J. (2007). The spectrum of power from wind turbines. *Journal of Power Sources*, 169(2), 369-374.

Archer, C. L., & Jacobson, M. Z. (2005). Evaluation of global wind power. *Journal of geophysical research*, 110(D12), D12110

Archer, C. L., & Jacobson, M. Z. (2007). Supplying Baseload Power and Reducing Transmission Requirements by Interconnecting Wind Farms. *Journal of Applied Meteorology and Climatology*, 46.

Borregaard, N. (2009). Opciones para la matriz eléctrica Chilena: Insumos para la discusión - Documento Resumen. Retrieved from [http://www.ffla.net/images/stories/PDFS/PUBLICACIONES/ffla\\_energia\\_chile.pdf](http://www.ffla.net/images/stories/PDFS/PUBLICACIONES/ffla_energia_chile.pdf)

Burton, T., Sharpe, D., Jenkins, N., & Bossanyi, E. (2001). *Wind Energy Handbook*. Chichester, New York: John Wiley and Sons Ltd.

CNE. (2008). Capacidad instalada por sistema eléctrico nacional Available from [http://www.cne.cl/cnewww/export/sites/default/06\\_Estadisticas/Documentos/capacidad\\_instalada\\_de\\_generacion.xls](http://www.cne.cl/cnewww/export/sites/default/06_Estadisticas/Documentos/capacidad_instalada_de_generacion.xls)

CNE. (2009a). Fijación de precios de nudo abril 2009 Sistema Interconectado Central (SIC). Informe Técnico Definitivo Available from [http://www.cne.cl/cnewww/opencms/07\\_Tarificacion/01\\_Electricidad/Otros/Precios\\_nudo/otros\\_precios\\_de\\_nudo/archivos\\_bajar/abril2009/ITD\\_SIC\\_ABR09.rar](http://www.cne.cl/cnewww/opencms/07_Tarificacion/01_Electricidad/Otros/Precios_nudo/otros_precios_de_nudo/archivos_bajar/abril2009/ITD_SIC_ABR09.rar)

CNE. (2009b). Fijacion de precios nudo abril 2009 Sistema Internecontado del Norte Grande (SING). Informe Técnico definitivo Available from

[http://www.cne.cl/cnewww/opencms/07\\_Tarificacion/01\\_Electricidad/Otros/Precios\\_nudo/otros\\_precios\\_de\\_nudo/archivos\\_bajar/abril2009/ITD\\_SING\\_ABR09.rar](http://www.cne.cl/cnewww/opencms/07_Tarificacion/01_Electricidad/Otros/Precios_nudo/otros_precios_de_nudo/archivos_bajar/abril2009/ITD_SING_ABR09.rar)

CNE. (2009c). Modelación del recurso solar y eólico en el norte de Chile. Retrieved from

<http://condor.dgf.uchile.cl/ViewerV2/EnergiaRenovable/datos/ModelacionRecursoSolarEolico1.pdf>

CNE. (2009d). Prospección eólica en zonas de las regiones de Atacama, de Coquimbo y del Maule (informe preliminar). Retrieved from

[http://www.cne.cl/cnewww/opencms/03\\_Energias/Otros\\_Niveles/renovables\\_noconvencionales/Tipos\\_Energia/eolica.html](http://www.cne.cl/cnewww/opencms/03_Energias/Otros_Niveles/renovables_noconvencionales/Tipos_Energia/eolica.html)

CNE. (2010). Explorador de energía eólica y solar. from

<http://condor.dgf.uchile.cl/ViewerV2/EnergiaRenovable/>

Czisch, G., & Ernst, B. (2001). High wind power penetration by the systematic use of smoothing effects within huge catchment areas shown in a European example, American Wind Energy Association Available from [http://www.iset.uni-kassel.de/abt/w3-w/projekte/awea\\_2001\\_czisch\\_ernst.pdf](http://www.iset.uni-kassel.de/abt/w3-w/projekte/awea_2001_czisch_ernst.pdf)

Giebel, v. G. (2000). On the Benefits of Distributed Generation of Wind Energy in Europe, Europe Ph.D. Dissertation, Carl von Ossietzky University of Oldenburgpp.

104). Available from

[http://www.drgiebel.de/GGiebel\\_DistributedWindEnergyInEurope.pdf](http://www.drgiebel.de/GGiebel_DistributedWindEnergyInEurope.pdf)

Inc, M. E. (2010). Windographer. from <http://www.windographer.com/>

inc., M. E. (2009). Windographer Database from Windographer Software.

Karki, R., & Po, H. (2005, 1-4 May 2005). *Wind power simulation model for reliability evaluation*. Paper presented at the Electrical and Computer Engineering, 2005. Canadian Conference on.

Katzenstein, W., Fertig, E., & Apt, J. (2010). The variability of interconnected wind plants. *Energy Policy*, 38(8), 4400-4410.

Kennedy, S., & Rogers, P. (2003). A Probabilistic Model for Simulating Long-Term Wind-Power Output. [10.1260/030952403769016654]. *Wind Engineering*, 27(3), 167-181.

Kirby, B., & Milligan, M. (2008). Facilitating Wind Development: The Importance of Electric Industry Structure. *The Electricity Journal*, 21(3), 40-54.

Milligan, M., & Porter, K. (2005). Determining the Capacity Value of Wind: A Survey of Methods and Implementation. *National Renewable Energy Laboratory*.

Noorgard, P. (2004). *A multi turbine Power Curve Approach*. Paper presented at the Nordic wind power conference. , Chalmers University of Technology.

Novoa, C., & Jin, T. (2011). Reliability centered planning for distributed generation considering wind power volatility. *Electric Power Systems Research*, 81(8), 1654-1661.

Peiyuan, C., Pedersen, T., Bak-Jensen, B., & Zhe, C. (2010). ARIMA-Based Time Series Model of Stochastic Wind Power Generation. *Power Systems, IEEE Transactions on*, 25(2), 667-676.

Poggi, P., Muselli, M., Notton, G., Cristofari, C., & Louche, A. (2003). Forecasting and simulating wind speed in Corsica by using an autoregressive model. *Energy Conversion and Management*, 44(20), 3177-3196.

SEIA. (2007). Informe Consolidado de la Evaluación de Impacto Ambiental de la Declaración de Impacto Ambiental del Proyecto "Parque Eólico Canela. Retrieved from <https://www.e-seia.cl/documentos/documento.php?idDocumento=1739862>

Spahic, E., Underbrink, A., Buchert, V., Hanson, J., Jeromin, I., & Balzer, G. (2009, June 28 2009-July 2 2009). *Reliability model of large offshore wind farms*. Paper presented at the PowerTech, 2009 IEEE Bucharest.

Vallee, F., Lobry, J., & Deblecker, O. (2007). Impact of the Wind Geographical Correlation Level for Reliability Studies. *Power Systems, IEEE Transactions on*, 22(4), 2232-2239.

Watts, D. (2009). Greenhouse Gass Emission Abatement in the Chilean Electricity Sector. .

Watts, D., & Jara, D. (2011). Statistical analysis of wind energy in Chile. *Renewable Energy*, 36(5), 1603-1613.